1948ApJ...107..151G

SPECTROPHOTOMETRY OF THE F STARS AND OF τ URSAE MAJORIS. I*

JESSE L. GREENSTEIN
Yerkes and McDonald Observatories
Received November 15, 1947

ABSTRACT

This investigation deals with the curves of growth and the abundances of the elements in a group of F stars of a wide range of luminosity. Line intensities of about three hundred and fifty lines have been measured on McDonald coudé spectra (Table 2) in τ UMa, ρ Pup, θ UMa, α CMi, and α Per. A discussion of central intensities shows that the spectrum of τ UMa, a "metallic-line A star," is not of binary composite origin. Hydrogen-line contours show only small dependence on luminosity in the F stars.

The theory of the curve of growth is examined from the point of view of model atmospheres. It is found that the use of a Milne-Eddington model with constant η appreciably changes the curves of growth from the Schuster-Schwarzschild model. An estimate is made, from models of a dwarf F star and of the sun, as to the actual variation of η with optical depth. In a comparison of the F stars with the sun some of these effects of stratification are partially eliminated. The deduced value of the damping constant in the sun and the F stars is much reduced by use of the M.E. model. Deviations from the theoretical curves of growth remain in the best-observed solar curve.

The semiempirical solar-line strengths of K. O. Wright are used to analyze the atmospheres of the five F stars. Similar empirical line strengths are derived from τ UMa. Curves of growth are given in Figures 1–10; the damping constants are low, and turbulence increases in the giant stars. From these curves the apparent abundances of the elements are derived for each star (Table 7). The temperature and pressure at a representative point in the atmospheres are determined by a simultaneous solution giving the correct level of ionization and opacity for some standard elements. This also yields the total pressure and surface gravity. After correction for level of ionization, the abundances relative to the sun of about twenty elements are given in Table 12. No well-established abundance changes by a factor of 2 exist (except in the peculiar star, τ UMa). In the mean the stellar and solar abundances are identical. A slight tendency exists in the supergiants for greater abundances of the heavier elements as compared to the dwarfs. An analysis of the hydrogen lines predicts the observed null-effect and suggests that the hydrogen/metal ratio is the same in the F stars as in the sun.

The present investigation is concerned with the effects of absolute magnitude on stellar spectra and with possible variations of the abundances of the elements from star to star. Even with the highest dispersion now available, the instrumental and physical blending of spectral lines is serious for all stars of types G and later. From a survey of available McDonald coudé spectra, it was found that stars of type F5 were most suitable for this investigation. One particular object of interest is the so-called "metallic-line A star," τ Ursae Majoris; since, in fact, τ UMa is a peculiar F star, a group of stars near F5 was chosen. The stars selected for analysis are standard stars in the Yerkes *Atlas of Stellar Spectra*.[1] The measures of α CMi and α Per were made in the *Photometric Atlas of Stellar Spectra*[2] and will be discussed in more detail by Greenstein and Hiltner[3] in Paper II of this series.

The McDonald coudé plates have a dispersion of 2.8 A/mm at $H\gamma$; the slit width ranges from 0.03 to 0.05 mm; and the resolution is near 30,000. Eastman 103*a*-O emulsion is used throughout. The spectral types and approximate luminosities are listed in Table 1, together with n, the number of measured tracings. Actually, θ UMa was measured on two completely independent microphotometer tracings of the same plate, reduced separately in a study of the accidental errors. Most lines were measured on three

* *Contributions from the McDonald Observatory, University of Texas,* No. 145.

[1] Morgan, Keenan, and Kellman (Chicago: University of Chicago Press, 1943).

[2] Hiltner and Williams (Ann Arbor, 1946).

[3] *Ap. J.*, in press; to be Paper II of this series.

plates in τ UMa; several different plates were used to obtain the intensity tracings in the *Photometric Atlas*[2] of α CMi and α Per, although few lines are measured on more than one plate.

The plates cover only the region $\lambda\lambda$ 4000–4800 A. The calibration, described elsewhere,[2] consists of a wedge-slit spectrogram taken with the coudé spectrograph and developed together with the stellar spectra under standard conditions. The final contrast, as measured on the microphotometer tracings, varies less than 10 per cent from night to night. The variation of contrast with wave length is very slow. A tube-photometer exposure is usually taken as a check on the wedge spectrogram; no systematic difference is found. The tracings obtained with the Yerkes microphotometer (which is of the conventional transmission type), have a dispersion of 35 mm/A. Line depths were measured every millimeter on the tracing, converted into absorptions, and numerically integrated to obtain the equivalent width. Overlap between successive tracings of a plate provided a check on the systematic agreement of individual runs. The extensive measures and reductions, involving about fifty thousand settings, were made with the kind assistance of Miss Gertrude Peterson, Mrs. Wrubel, and Mrs. Greenstein. About three hundred and fifty lines were chosen for measurement. Identifications are based mainly

TABLE 1

STARS MEASURED SPECTROPHOTOMETRICALLY

Star	Abs. Mag.	Type	n	Line Quality
τ UMa.	+3:	F6+A3	4	Broadened
α Per.	−5	F5 I*b*	1	Very broad
ρ Pup.	−3	F6 II	2	Broadened
θ UMa.	+1.5	F6 III	2	Sharp
α CMi.	+2.5	F5 IV	1	Sharp

on Swensson's study[4] of α CMi but take account of the strengthening of the ionized elements in high-luminosity objects. For use, a line should be substantially unblended in the sun, in α CMi, and in the supergiants. Unfortunately, the increased strength of the lines and the turbulent broadening in α Per, τ UMa, and ρ Pup makes blending serious; many useful lines had to be omitted in α Per. The lines selected had, in general, solar values of the line-absorption coefficient, log X_f, available in an unpublished list by Dr. K. O. Wright, of the Dominion Astrophysical Observatory, who very kindly supplied his data prior to publication. A group of rare-earth and other important lines was added, many of which were weak, blended, or absent in the sun. For some lines new values of the solar log X_f were determined; unfortunately, some could be derived only from the Rowland estimated intensities.

Table 2 gives the spectrophotometric measures of $-\log_{10} W/\lambda$. The wave lengths used are the laboratory values. A symbol p (or a single dot in the figures) indicates that the measurements are affected by blending on the tracings; the symbol P (or a double dot in the figures) indicates serious blending and very low weight. The excitation potentials, E.P., in electron-volts, are given for the lower level producing the line. The value of log $\eta_0(\tau)$ is given for each line in τ UMa; analogous to the solar log X_0, it is the ratio at the center of the line of s_0, the line-absorption coefficient to the continuous-absorption coefficient, κ_ν. The $\eta_0(\tau)$ is read from the theoretical curve of growth of τ UMa, using the measured intensity in that star. While the measured intensities are inferior in accuracy to the solar values and while τ UMa is a peculiar star, these $\eta_0(\tau)$'s have considerable usefulness. In analysis of A and F stars many lines of ionized elements, especially rare

[4] *Ap. J.*, **103**, 207, 1946.

1948ApJ...107..151G

TABLE 2

MEASURED LINE INTENSITIES IN F STARS

$-\log W/\lambda$

λ	Element	τ UMa	ρ Pup	θ UMa	α CMi	α Per	log $\eta_0(\tau)$*	E.P.	Notes
4017.16	*Fe* I	4.44p	....	....	4.49	....	1.52	3.04	
20.90	*Co* I	4.75	....	....	4.79	4.84p	0.60	0.43	
22.74	*Fe* I	4.86p	....	....	4.75P	....	0.38	3.27	
28.33	*Ti* II	4.41p	....	....	4.50	4.14	1.65	1.88	
33.07	*Mn* I	4.21p	....	....	4.24p	4.01P	2.80	0	
34.49	*Mn* I	4.31	....	....	4.38	4.08	2.20	0	
35.73	*Mn* I	4.23p	....	....	4.29	4.06	2.67	2.13	1
36.78	*V* II	4.69	....	....	4.61	4.43p	0.75	1.47	
40.65	*Fe* I	4.29	....	....	4.49	4.35P	2.30	3.27	
41.36	*Mn* I	4.35	....	....	4.37	4.22P	1.95	2.11	
44.61	*Fe* I	4.35	....	....	4.41	4.34p	1.95	2.82	
45.82	*Fe* I	3.83p	....	3.97	3.88	3.72P	....	1.48	1
47.32	*Fe* I	5.33P	....	5.65P	5.09P	5.01P	9.70	2.27	
49.33	*Fe* I	4.76	....	4.97p	4.88P	....	0.58	2.58	
50.32	*Zr* II	5.52	....	5.35	4.81P	....	9.48	0.71	
55.54	*Mn* I	4.48P	....	4.61	4.50	4.56p	1.37	2.13	
57.50	*Mg* I	4.30p	4.19p	4.28	4.15	4.19p	2.25	4.33	1
59.39	*Mn* I	5.05	5.31P	5.19P	5.16p	....	0.08	3.06	
59.73	*Fe* I	4.65p	4.73p	4.87	4.87	....	0.85	3.53	
62.82	*Pr* II	4.66P	4.91p	5.28p	5.50P	....	0.82	0.42	1, 2
63.60	*Fe* I	4.18p	4.06p	4.20p	3.97p	3.95P	2.95	1.55	
65.07	*V* II	4.85	4.93	5.15p	4.94P	....	0.40	3.78	2
65.39	*Fe* I	4.88	4.84P	4.93p	4.57p	....	0.35	3.42	
67.98	*Fe* I	4.38	4.30	4.55	4.42	4.25	1.80	3.20	
70.77	*Fe* I	4.46p	4.48p	4.69	4.50	4.37p	1.44	3.23	
71.74	*Fe* I	4.11	4.08	4.16	4.10	3.99	3.28	1.60	
72.52	*Fe* I	4.55	4.62	4.80	4.56	4.40	1.13	3.42	
73.48	*Ce* II	4.70P	4.80P	5.38P	5.35P	....	0.72	0	
77.71	*Sr* II	3.88	3.85p	4.15	4.02	3.75P	4.00	0	1
79.85	*Fe* I	4.58	4.53p	4.72	4.56	....	1.03	2.85	
82.94	*Mn* I	4.61p	4.57	4.80	4.56	....	0.95	2.17	
83.23	*Ce* II	4.72p	4.92	5.21p	5.31P	....	0.67	1.30	
84.50	*Fe* I	4.43	4.43P	4.61	4.43	4.41p	1.56	3.32	
86.72	*La* II	4.61p	4.56P	4.91	4.77	....	0.95	0	
91.56	*Fe* I	4.95	4.84	4.95	4.94	4.73P	0.23	2.82	3
4109.07	*Fe* I	4.80	4.70p	4.86	4.75	....	0.50	3.28	3
10.53	*Co* I	4.62	4.80	4.82p	4.92	4.82P	0.92	1.04	3
11.78	*V* I	4.79	4.86p	4.87	4.86	4.86p	0.52	0.30	3
12.35	*Fe* I	5.00p	....	4.96p	4.96	4.82P	0.15	3.38	3
14.45	*Fe* I	4.59	4.54p	4.70	4.61	4.50	1.00	2.82	3
15.18	*V* I	4.90P	4.87P	5.09P	4.95P	4.81P	0.32	0.28	3
18.14	*Ce* II	4.87P	4.91P	5.27P	5.18P	....	0.37	0.22	
18.77	*Co* I	4.39P	4.33P	4.49P	4.43P	....	1.75	1.04	1
20.83	*Ce* II	4.97	5.11p	5.47p	5.61P	4.84P	0.20	0.92	
21.32	*Co* I	4.48	4.43	4.62	4.44	4.37P	1.37	0.92	
23.23	*La* II	4.51p	4.50P	4.89	4.75P	4.38P	1.27	0.32	
26.19	*Fe* I	4.57p	4.43P	4.70	4.53P	....	1.06	3.32	
26.52	*Cr* I	4.91p	....	5.29	5.06p	....	0.30	2.53	
28.05	*Si* II	4.38p	4.35P	4.64P	4.46p	4.15P	1.80	9.79	2, 4
28.74	*Fe* II	4.50p	4.44p	4.82	4.64	4.24P	1.30	2.57	

* When log $\eta_0(\tau)$ is negative it is given in the form log $\eta_0(\tau) + 10$.

TABLE 2—*Continued*

λ	Element	τ UMa	ρ Pup	θ UMa	α CMi	α Per	log $\eta_0(\tau)$	E.P.	Notes
4129.73	*Eu* II	4.38P	4.35p	4.93P	4.77P	4.51P	1.80	0	5
32.06	*Fe* I	4.14p	4.11P	4.28	4.21	....	3.15	1.60	
32.90	*Fe* I	4.45p	4.40P	4.63	4.45p	....	1.48	2.82	
33.87	*Fe* I	4.40p	4.40p	4.64p	4.43p	4.34	1.70	3.42	1
36.51	*Fe* I	4.79p	4.74p	4.90	4.54	....	0.52	3.35	
37.00	*Fe* I	4.40	4.36	4.64	4.46	4.46P	1.70	3.40	
39.93	*Fe* I	4.84	4.78	4.91	4.76	4.73	0.42	0.99	
40.44	*Fe* I	4.80	4.76	4.96	4.75	4.80p	0.50	3.40	
43.42	*Fe* I	4.31	4.24P	4.42	4.39	4.21P	2.20	3.03	
43.87	*Fe* I	4.23	4.16p	4.32	4.26	4.09P	2.67	1.55	
47.67	*Fe* I	4.43	4.36p	4.59	4.46	4.30p	1.56	1.48	
50.97	*Zr* II	4.65	4.58	4.91P	4.89	4.44	0.85	0.80	1
57.79	*Fe* I	4.36	4.34	4.58	4.44	4.27	1.90	3.40	
61.20	*Zr* II	4.51p	4.36p	4.63p	4.53P	....	1.27	0.71	
61.80	*Sr* II	4.52P	4.45p	4.95p	4.77P	....	1.23	2.93	
66.00	*Ba* II	4.70	4.93	5.34	5.47P	....	0.72	2.71	
67.27	*Mg* I	4.38p	4.26p	4.38	4.24p	4.09p	1.80	4.33	
72.75	*Fe* I	....	....	4.35	....	4.17P	......	0.95	1
74.92	*Fe* I	4.49	4.41	4.60	4.42	4.38P	1.33	1.00	
75.64	*Fe* I	4.37	4.28	4.59	4.36	4.25p	1.85	2.83	
77.54	*Y* II	4.04	4.02	4.27	4.19	3.95p	3.53	0.41	
78.39	*V* II	4.80p	4.90p	5.22p	5.09p	....	0.50	1.68	
78.86	*Fe* II	4.23P	4.22p	4.55	4.36	3.92P	2.67	2.57	
79.81	*Zr* II	5.32P	4.91	5.37	5.30p	....	9.71	1.66	
83.44	*V* II	4.56	4.58	4.85	4.55p	4.31P	1.10	2.04	
84.90	*Fe* I	4.40	4.37	4.61	4.54	4.33P	1.70	2.82	
86.60	*Ce* II	4.53	4.54p	4.86p	4.83p	....	1.20	0.38	
87.04	*Fe* I	4.27p	4.23p	4.43	4.34	....	2.40	2.44	
87.80	*Fe* I	4.16	4.11	4.36p	4.23P	4.03p	3.05	2.42	
92.07	*Ni* II	4.65	4.87p	4.84p	5.05	4.68P	0.85	4.01	2
99.10	*Fe* I	4.27	4.19	4.47	4.38	4.11P	2.40	3.03	
99.97	*Fe* I	4.76	4.71	4.77p	4.59p	4.74P	0.58	0.09	1
4200.93	*Fe* I	4.51	4.43	4.67P	4.44P	4.37P	1.27	3.38	
03.99	*Fe* I	4.32	4.27	4.52	4.39	4.16p	2.14	2.83	
04.69	*Y* II	4.64P	4.62P	4.87P	4.78P	....	0.87	0	2
05.05	*Eu* II	4.29p	4.30P	4.62P	4.63P	4.28P	2.30	0	2, 5
06.38	*Mn* II	4.89P	4.99	5.45p	5.35P	....	0.34	5.37	2
06.70	*Fe* I	4.55p	4.52P	4.59	4.48p	4.29P	1.13	0.05	
07.35	*Cr* II	4.78P	4.93p	5.09p	5.19P	....	0.54	3.81	2
08.99	*Zr* II	4.85p	4.49P	4.81	4.76p	....	0.40	0.71	
10.35	*Fe* I	4.33	4.24	4.47	4.42	4.22p	2.07	2.47	
13.65	*Fe* I	4.52	4.43	4.69p	4.56	4.42	1.23	2.82	
15.02	*Gd* II	4.85	5.01	5.06	5.72P	....	0.40	0.43	2
15.52	*Sr* II	4.03	3.98	4.21p	4.15	3.93p	3.56	0	
16.19	*Fe* I	4.37	4.30	4.48p	4.38	4.24P	1.85	0	
19.36	*Fe* I	4.30	4.22	4.65	4.37	4.24	2.25	3.56	
22.22	*Fe* I	4.35	4.28	4.52	4.45	....	1.95	2.44	
22.98	*Pr* II	4.98P	5.06p	5.10p	5.28P	....	0.18	0.05	2
26.73	*Ca* I	4.19P	4.00p	4.07P	3.98p	4.00P	2.90	0	
27.43	*Fe* I	4.21	4.11p	4.34	4.21p	4.10P	2.80	3.32	

TABLE 2—*Continued*

λ	Element	τ UMa	ρ Pup	θ UMa	α CMi	α Per	log $\eta_0(\tau)$	E.P.	Notes
4228.72......	*Fe* I	5.35p	5.28P	5.51P	5.45	....	9.68	3.35	
32.06......	*V* II	4.83P	4.84p	5.15p	5.02p	....	0.44	3.96	2
33.17......	*Fe* II	4.19P	4.12P	4.41	4.29	....	2.90	2.57	1
33.61......	*Fe* I	4.31p	4.25P	4.47	4.39	....	2.20	2.47	
35.94......	*Fe* I	4.17	4.12	4.28	4.26	4.05p	3.00	2.42	
38.03......	*Fe* I	4.56p	4.46p	4.63	4.57	....	1.10	3.40	
38.38......	*La* II	4.54P	4.74P	5.02P	5.40P	....	1.16	0.40	
40.37......	*Fe* I	4.81p	4.59	4.67	4.56p	4.82P	0.48	3.53	
44.26......	*Mn* II	5.33	5.72	5.45	5.85	5.16P	9.70	5.35	
44.80......	*Ni* II	4.69	5.02	5.48	5.48	5.00P	0.75	4.02	
45.26......	*Fe* I	4.41	4.35	4.47	4.41	4.43p	1.65	2.85	
46.09......	*Fe* I	4.48	4.49	4.66	4.65	4.47p	1.37	3.63	
46.83......	*Sc* II	4.31p	4.20	4.40	4.33	4.04P	2.20	0.31	
47.43......	*Fe* I	4.32	4.29	4.42	4.37	4.13p	2.14	3.35	
48.23......	*Fe* I	4.54	4.51p	4.64p	4.51	4.49P	1.16	3.06	
48.68......	*Ce* II	4.72	4.92p	4.93P	5.12P	....	0.67	0.20	2
50.12......	*Fe* I	4.29	4.23	4.41	4.38	4.11p	2.30	2.46	
50.79......	*Fe* I	4.25	4.16	4.33	4.31	4.06p	2.54	1.55	
51.74......	*Gd* II	4.68p	4.83	5.35	5.45	....	0.77	0.38	2
52.62......	*Cr* II	4.41p	4.51	4.82	4.76	4.29P	1.65	3.84	
54.35......	*Cr* I	4.20	4.18	4.38	4.37	4.06	2.85	0	
58.62......	*Fe* I	5.02p	4.95P	4.85P	4.81P	....	0.12	2.82	
60.48......	*Fe* I	4.19	4.09P	4.29P	4.10P	....	2.90	2.39	
61.92......	*Cr* II	4.32p	4.33	4.59p	4.49p	4.17	2.14	3.85	
63.59......	*La* II	4.89p	5.03P	5.32	5.55P	....	0.34	1.95	2
64.21......	*Fe* I	4.83p	4.72p	4.80	4.73	4.69P	0.44	3.35	
64.74......	*Fe* I	5.10	4.95p	5.04	4.96	....	0.00	3.94	
65.26......	*Fe* I	4.87	4.73	4.96	4.86	4.76P	0.37	3.91	
67.83......	*Fe* I	4.58	4.46	4.58	4.45	4.48	1.03	3.10	
71.16......	*Fe* I	4.30	4.23	4.38	4.35	4.13P	2.25	2.44	
71.76......	*Fe* I	4.18	4.08	4.19	4.15	4.02P	2.95	1.48	
74.80......	*Cr* I	4.24	4.18	4.35	4.26	4.12p	2.60	0	
76.68......	*Fe* I	4.84	4.77P	5.01	4.90	4.64P	0.42	3.86	
82.41......	*Fe* I	4.29	4.21	4.48	4.41	4.08p	2.30	2.17	
83.01......	*Ca* I	4.70	4.32	4.49	4.42	4.20P	0.72	1.88	
83.77......	*Mn* II	5.33p	5.52	5.90p	5.68P	....	9.70	5.35	2
84.21......	*Cr* II	4.44	4.44P	4.73	4.58	4.18p	1.52	3.84	
85.44......	*Fe* I	4.56	4.45p	4.58	4.55	4.52p	1.10	3.22	
86.01......	*Ti* I	5.00P	4.75P	4.64P	4.65p	....	0.15	0.82	
86.97......	*La* II	4.54	4.62	4.62	4.45	....	1.16	1.94	1
87.40......	*Ti* I	5.24	5.00	4.99	4.93	....	9.81	0.83	
89.07......	*Ti* I	5.00P	....	4.74P	....	....	0.15	0.82	
90.93......	*Ti* I	4.78	....	4.52P	....	4.78P	0.54	0.81	1
91.47......	*Fe* I	4.75	4.61	4.77p	4.65	4.63P	0.60	0.05	
94.77......	*Sc* II	4.95	4.65	4.69	4.60	....	0.23	0.60	
96.57......	*Fe* II	4.21	4.18	4.46p	4.42	4.03P	2.80	2.69	
98.66......	*Ti* I	4.90	4.73P	4.58P	4.78P	....	0.32	0.82	
4300.05......	*Ti* II	4.19p	4.05p	4.30p	4.24p	3.92P	2.90	1.18	
00.82......	*Fe* I	4.92p	....	4.62P	4.64P	....	0.28	3.97	
01.93......	*Ti* II	4.24p	4.17P	4.43P	4.40p	....	2.60	1.16	

TABLE 2—*Continued*

λ	Element	τ UMa	ρ Pup	θ UMa	α CMi	α Per	log $\eta_0(\tau)$	E.P.	Notes
4302.53......	*Ca* I	4.53p	4.23P	4.37P	4.37p	....	1.20	1.89	1
03.17......	*Fe* II	4.30p	4.21p	4.52P	4.43p	....	2.25	2.69	
03.57......	*Nd* II	4.61p	4.71	4.75P	4.93P	....	0.95	0	
12.86......	*Ti* II	4.31	4.21	4.36	4.29	4.06	2.20	1.18	
16.06......	*Gd* II	5.11	5.24	5.43	5.79P	4.91P	9.99	0.66	1, 2
16.81......	*Ti* II	4.65	4.49p	4.73	4.65	4.16p	0.85	2.04	
17.32......	*Zr* II	5.22	4.85	5.02	5.19p	....	9.84	0.71	
18.65......	*Ca* I	4.69	4.36	4.50	4.41	4.14	0.75	1.89	
22.51......	*La* II	4.96	5.20	5.43	5.79	4.60P	0.22	0.17	
25.01......	*Sc* II	4.48p	4.29	4.37	4.33	4.12p	1.37	0.59	3
25.76......	*Fe* I	4.09p	4.01	4.16	4.12	4.13p	3.36	1.60	3
30.26......	*Ti* II	4.69P	4.55	4.76P	4.81	....	0.75	2.04	3
33.28......	*Zr* II	5.09p	5.00p	5.29p	5.46P	....	0.02	2.40	3
33.76......	*La* II	4.46	4.57	4.81	5.06p	4.64p	1.44	0.17	3
37.05......	*Fe* I	4.51p	4.33P	4.48	4.57	4.48P	1.27	1.55	3
52.74......	*Fe* I	4.41	4.34	4.45	4.50	4.43	1.65	2.21	3
54.61......	*Sc* II	4.77	4.67p	4.67p	4.66	4.53p	0.56	0.60	3
55.10......	*Ca* I	5.10	4.70	4.70	4.56	4.75P	0.00	2.70	3
58.17......	*Nd* II	4.80p	4.95	5.22	5.74P	....	0.50	0.32	
62.10......	*Ni* II	4.58	4.71	5.05	4.85	4.55P	1.03	4.01	
69.40......	*Fe* II	4.51P	4.45P	4.83p	4.56p	....	1.27	2.77	
71.28......	*Cr* I	4.60	4.64P	4.62p	4.51p	....	0.97	1.00	
74.46......	*Sc* II	4.62P	4.38	4.49p	4.48	....	0.92	0.62	
74.94......	*Y* II	4.23	4.18P	4.42P	4.44	....	2.67	0.41	1, 2
75.93......	*Fe* I	4.33	4.32	4.51	4.42	4.19	2.07	0.02	
79.24......	*V* I	4.79	4.67	4.65	4.63	....	0.52	0.30	
82.17......	*Ce* II	4.81	4.92	5.16	5.56P	....	0.48	0.20	
83.55......	*Fe* I	4.13	4.06	4.09	4.11	4.14	3.20	1.48	
85.38......	*Fe* II	4.23P	4.17P	4.46p	4.36P	....	2.67	2.77	
87.90......	*Fe* I	4.62	4.54p	4.70p	4.63	....	0.92	3.06	
88.41......	*Fe* I	4.48	4.36p	4.60	4.50	....	1.37	3.59	
89.24......	*Fe* I	5.07	4.82	4.89	4.78p	5.00P	0.05	0.05	
89.97......	*V* I	4.80p	4.71p	4.72	4.80P	....	0.50	0.27	
90.58......	*Mg* II	4.86P	4.80P	4.87	....	....	0.38	9.96	1, 2
92.58......	*Fe* I	5.12	4.97P	5.15	4.94P	5.18	9.97	3.86	
94.06......	*Ti* II	4.47	4.35	4.50	4.42	4.28	1.40	1.22	
95.03......	*Ti* II	4.14	4.09	4.24	4.21	4.00	3.15	1.08	
95.85......	*Ti* II	4.54	4.38	4.59	4.50	4.20p	1.16	1.24	
98.02......	*Y* II	4.47	4.35P	4.73p	4.67	....	1.40	0.13	
99.77......	*Ti* II	4.30	4.23	4.39	4.37	4.05p	2.25	1.23	
4400.36......	*Sc* II	4.68p	4.34p	4.43	4.44	4.11P	0.77	0.60	
04.75......	*Fe* I	4.18	4.07	4.15	4.16	4.06	2.95	1.55	
06.64......	*V* I	4.97	4.94	4.83	5.04P	5.05P	0.20	0.30	
08.84......	*Pr* II	4.85P	5.02P	5.21P	5.77P	....	0.40	0	1, 2
10.52......	*Ni* I	4.60p	4.71	4.92P	4.79	....	0.97	3.29	
11.94......	*Ti* II	4.70p	4.56	4.78	4.60	4.21	0.72	1.22	
15.12......	*Fe* I	4.16	4.07p	4.26	4.25	....	3.05	1.60	
15.56......	*Sc* II	4.82P	4.36	4.54p	4.51P	....	0.46	0.59	
16.82......	*Fe* II	4.29	4.21	4.52	4.42	4.12	2.30	2.77	
17.72......	*Ti* II	4.30	4.21	4.50	4.37	4.09p	2.25	1.16	

TABLE 2—*Continued*

λ	Element	τ UMa	ρ Pup	θ UMa	α CMi	α Per	log $\eta_0(\tau)$	E.P.	Notes
4418.34	*Ti* II	4.55	4.40P	4.63	4.56	....	1.13	1.23	
21.95	*Ti* II	4.63	4.46	4.69p	4.57	4.29p	0.90	2.05	
24.34	*Sm* II	4.61	4.71	4.83	5.04P	....	0.95	0.48	1, 2
25.44	*Ca* I	4.69	4.33	4.46	4.42	4.31	0.75	1.87	
27.31	*Fe* I	4.29	4.17	4.34p	4.31p	4.23	2.30	0.05	
28.00	*Mg* II	4.86	4.88P	5.09p	5.16P	4.67P	0.38	9.95	1, 2
30.62	*Fe* I	4.38	4.30p	4.44p	4.40p	....	1.80	2.21	
31.37	*Sc* II	5.17P	4.99	4.85	4.87	4.67p	9.91	0.60	
32.57	*Fe* I	4.89p	4.80P	4.97	4.83	....	0.34	3.56	
33.22	*Fe* I	4.48	4.46P	4.58	4.54	4.61p	1.37	3.00	
34.32	*Sm* II	4.76	4.77	5.00	5.04	....	0.58	0.38	
35.69	*Ca* I	4.42P	4.32p	4.45	4.49	4.35P	1.61	1.88	1
37.57	*Ni* I	4.82	5.00	5.08p	4.81P	5.13	0.46	3.66	
38.35	*Fe* I	4.86	4.83	4.89p	4.78P	5.05p	0.38	3.67	
42.34	*Fe* I	4.36	4.29	4.45	4.44	4.33P	1.90	2.19	
43.80	*Ti* II	4.23	4.17	4.38	4.32	4.20P	2.67	1.08	
47.72	*Fe* I	4.37	4.31	4.48p	4.39	4.29	1.85	2.21	
55.89	*Ca* I	4.62	4.40	4.47	4.41	4.35p	0.92	1.89	
57.43	*Ti* I	4.65	4.52p	4.57p	4.59	4.54p	0.85	1.45	1, 2
62.98	*Nd* II	4.76	4.88	5.02	5.54P	....	0.58	0.56	
65.81	*Ti* I	5.13p	5.09	5.12	5.29p	5.12P	9.96	1.73	
66.55	*Fe* I	4.30	4.24	4.48	4.42	4.24	2.25	2.82	
67.34	*Sm* II	4.73p	4.92	5.16	5.61P	....	0.65	0.66	
68.49	*Ti* II	4.24	4.17	4.38	4.30	4.13	2.60	1.13	
72.92	*Fe* II	4.29	4.27	4.50p	4.42p	4.16	2.30	2.83	
76.02	*Fe* I	4.30	4.27	4.43	4.36	4.20	2.25	2.83	
79.61	*Fe* I	4.60P	4.62P	4.85p	4.65P	4.67P	0.97	3.67	
80.14	*Fe* I	4.60p	4.55P	4.67P	4.58P	4.66P	0.97	3.03	
81.13	*Mg* II	3.99	3.97	4.27	4.12	3.90	3.70	8.82	
84.23	*Fe* I	4.51	4.47	4.73	4.64	4.45p	1.27	3.59	
85.68	*Fe* I	4.66	4.62	4.77	4.75	4.59	0.82	3.67	
88.32	*Ti* II	4.41	4.40	4.59p	4.52	4.28	1.65	3.11	
89.18	*Fe* II	4.26	4.24	4.52	4.44p	4.13p	2.47	2.82	
89.74	*Fe* I	4.75p	4.63P	4.70	4.69p	....	0.60	0.12	
90.08	*Fe* I	4.78	....	4.84p	....	....	0.54	3.00	
91.40	*Fe* II	4.31	4.29	4.59	4.46	4.20	2.20	2.84	
93.53	*Ti* II	4.81	4.83	4.93	4.91	....	0.48	1.08	1
94.06	*Fe* I	5.04p	5.00P	5.08p	4.99P	....	0.09	3.97	
94.57	*Fe* I	4.35	4.26	4.44	4.39	4.16	1.95	2.19	
95.97	*Fe* I	4.99	5.00P	5.15P	5.21P	5.08P	0.17	3.64	
4501.27	*Ti* II	4.24	4.18	4.36	4.34	4.16	2.60	1.11	
02.22	*Mn* I	4.91p	4.87	5.04	5.06	....	0.30	2.91	
04.84	*Fe* I	5.03	4.96	5.00p	5.09P	5.03	0.11	3.25	
06.74	*Ti* II	5.09P	5.07	5.03p	5.06P	....	0.02	1.13	1
08.28	*Fe* II	4.23	4.22	4.51	4.40	4.04	2.67	2.84	
10.21	*Mn* II	5.19	5.44	5.51p	....	....	9.88	10.61	1, 2
12.73	*Ti* I	4.83p	5.00	4.80p	4.98	4.88	0.44	0.83	
15.34	*Fe* II	4.22	4.22	4.50	4.43	4.05	2.74	2.83	
17.53	*Fe* I	4.79p	4.86	4.89	4.89	5.06P	0.52	3.06	
20.23	*Fe* II	4.23	4.24	4.48	4.38	4.10	2.67	2.80	

TABLE 2—*Continued*

λ	Element	τ UMa	ρ Pup	θ UMa	α CMi	α Per	log $\eta_0(\tau)$	E.P.	Notes
4522.63......	*Fe* II	4.09	4.10	4.29	4.30	3.95	3.36	2.83	1
28.62......	*Fe* I	4.13	4.15	4.25	4.28	4.07	3.20	2.17	1
29.46......	*Ti* II	4.32	4.30	4.40	4.38	4.17	2.14	1.56	1
31.63......	*Fe* I	4.93	4.92	4.98	4.97	....	0.27	3.20	
34.78......	*Ti* I	4.89p	4.67	4.71	4.71	4.75P	0.34	0.83	
41.52......	*Fe* II	4.28	4.26	4.59	4.53	4.20	2.35	2.84	
45.14......	*Ti* II	4.59p	4.47p	4.65p	4.72	....	1.00	1.13	
45.96......	*Cr* I	4.62	4.63	4.73	4.68	....	0.92	0.94	
48.76......	*Ti* I	5.17	4.87P	4.87P	4.99	5.06P	9.91	0.82	
51.24......	*Ni* I	4.87p	4.92P	5.09P	5.29	5.26P	0.37	4.15	
54.03......	*Ba* II	4.14	4.11	4.31	4.38	4.12	3.15	0	
55.02......	*Cr* II	4.39	4.38	4.77	4.74	4.37p	1.75	4.05	
58.66......	*Cr* II	4.19	4.17	4.50	4.42	4.07	2.90	4.06	
62.36......	*Ce* II	4.64	4.75	4.94	5.21	4.61	0.87	0	
63.76......	*Ti* II	4.27	4.15	4.43p	4.35	4.05	2.40	1.22	
64.59......	*V* II	4.54P	4.60	4.84p	4.80	4.58	1.16	2.26	1
68.31......	*Ti* II	5.12	4.80P	4.97	4.84p	....	9.97	1.22	
71.10......	*Mg* I	5.15	4.79	4.76	4.67	4.79p	9.93	0	1
71.97......	*Ti* II	4.08	4.06	4.34	4.20	3.94	3.40	1.56	
76.33......	*Fe* II	4.34	4.33	4.71	4.53	4.23	2.00	2.83	
78.56......	*Ca* I	5.02	4.73	4.67	4.64	4.67	0.12	2.51	
82.84......	*Fe* II	4.37P	4.37p	4.72	4.66	....	1.85	2.83	
83.83......	*Fe* II	4.15	4.06	4.40	4.43	4.04p	3.10	2.80	
85.87......	*Ca* I	4.96P	4.51p	4.57	4.52	4.48p	0.22	2.52	
86.36......	*V* I	....	4.95P	5.12P	....	....	......	0.04	1
87.13......	*Fe* I	4.82	4.85	5.02	4.82	4.91	0.46	3.56	
88.22......	*Cr* II	4.27	4.27	4.60	4.47	4.14	2.40	4.05	
91.39......	*Cr* I	4.67	4.69p	4.79	4.64	....	0.80	0.96	
92.09......	*Cr* II	4.38P	4.42p	4.84	4.62	....	1.80	4.06	
96.06......	*Fe* I	4.53p	....	4.76p	....	....	1.20	3.59	
96.98......	*Gd* II	4.88p	5.02	5.13	5.20P	....	0.35	0.52	2
97.91......	*Gd* II	4.65P	4.68P	4.93P	4.99P	....	0.85	0.60	2
4602.01......	*Fe* I	4.85	4.72	4.85	4.86	4.89	0.40	1.60	
02.94......	*Fe* I	4.44	4.36	4.56	4.51	4.29	1.52	1.48	
04.99......	*Ni* I	4.47P	4.53p	4.78	4.64	....	1.40	3.46	
11.28......	*Fe* I	4.40	4.37	4.55	4.51	4.46	1.70	0.91	
16.14......	*Cr* I	4.60p	4.75p	4.77	4.74	....	0.97	0.98	
16.64......	*Cr* II	4.41p	4.49p	4.91	4.74	....	1.65	4.06	
17.27......	*Ti* I	5.19	5.10	4.99	4.96	5.08P	9.88	1.74	
19.87......	*La* II	5.01p	5.34	5.70	5.74	....	0.14	1.75	2
20.51......	*Fe* II	4.45	4.41	4.75	4.72	4.27	1.48	2.82	
25.05......	*Fe* I	4.48	4.49	4.70	4.70	4.57	1.37	3.23	
28.16......	*Ce* II	4.63	4.82	5.03	5.43	4.75	0.90	0.04	
32.92......	*Fe* I	4.63	4.58	4.65	4.64	4.66	0.90	1.60	
34.11......	*Cr* II	4.35	4.38	4.68	4.59	4.24	1.95	4.06	
37.51......	*Fe* I	4.60	4.52P	4.73	4.69	....	0.97	3.27	
38.02......	*Fe* I	4.56	4.51P	4.70	4.69	....	1.10	3.59	
42.24......	*Sm* II	5.10	5.12	5.49	....	....	0.00	0.38	2
43.47......	*Fe* I	4.65	4.54	4.79p	4.81	4.67p	0.85	3.64	
46.17......	*Cr* I	4.42p	4.38p	4.62	4.66	4.43p	1.60	1.03	

λ	Element	τ UMa	ρ Pup	θ UMa	α CMi	α Per	log $\eta_0(\tau)$	E.P.	Notes
4647.44......	*Fe* I	4.43p	4.38p	4.63	4.63	4.52p	1.56	2.94	
48.66......	*Ni* I	4.33	4.33	4.68p	4.59	4.46P	2.07	3.41	
51.28......	*Cr* I	4.60p	4.67	4.82	4.85	4.72	0.97	0.98	
52.16......	*Cr* I	4.54	4.54p	4.73	4.68	4.51	1.16	1.00	
62.51......	*La* II	4.90	4.95P	5.41p	5.41P	4.91P	0.32	0	
68.14......	*Fe* I	4.50p	4.44p	4.60	4.62p	4.51P	1.30	3.25	
68.56......	*Na* I	4.87p	4.88	5.26p	5.38p	....	0.37	2.10	1
73.17......	*Fe* I	4.60	4.50	4.70	4.62p	4.74	0.97	3.64	
74.60......	*Sm* II	4.76p	4.93	5.14	5.41p	....	0.58	0.18	1, 2
76.91......	*Sm* II	5.22	5.19	5.59	5.56	....	9.84	0.04	2
82.32......	*Y* II	4.68P	4.55	5.03p	4.86P	....	0.77	0.41	2
86.22......	*Ni* I	4.61	4.67	5.01	4.95	4.98p	0.95	3.58	
94.13......	*S* I	4.78	4.77	5.09	5.08p	4.86	0.54	6.50	1, 2
95.45......	*S* I	5.05P	4.98P	5.40P	5.31p	5.10P	0.08	6.50	2
96.25......	*S* I	5.22P	5.21	5.59	5.63p	5.39	9.84	6.50	2
4702.99......	*Mg* I	4.30	4.19	4.32	4.23	4.12	2.25	4.33	
03.81......	*Ni* I	4.56	4.71p	5.05	4.86	5.09P	1.10	3.64	
04.96......	*Fe* I	4.83p	4.71p	4.95	4.86p	....	0.44	3.67	
05.46......	*Fe* I	5.15	5.13p	5.13	5.22	....	9.93	3.53	
07.28......	*Fe* I	4.39	4.37	4.51	4.48	4.48	1.75	3.23	
10.29......	*Fe* I	4.52	4.60	4.70	4.64	4.89p	1.23	3.00	
14.42......	*Ni* I	4.24p	4.24	4.52	4.44	4.37	2.60	3.36	
15.78......	*Ni* I	4.46	4.53	4.79	4.74	4.72	1.44	3.53	
22.16......	*Zn* I	4.43	4.51	4.73	4.68	4.80	1.56	4.01	
30.03......	*Mg* I	4.80P	4.72P	4.78P	5.18P	....	0.50	4.33	
31.44......	*Fe* II	4.29P	4.27	4.58	4.51	4.19	2.30	2.88	
33.60......	*Fe* I	4.68p	4.65p	4.69	4.78	4.68p	0.77	1.48	
35.85......	*Fe* I	4.78	4.73	4.88	4.93	5.04	0.54	4.C6	
36.78......	*Fe* I	4.34p	4.32p	4.51	4.58p	....	2.00	3.20	
45.81......	*Fe* I	4.70	4.54	4.80	4.80	4.75	0.72	4.09	
48.73......	*La* II	4.97p	5.19p	5.31	5.68	5.33P	0.20	0.92	
54.04......	*Mn* I	4.48	4.40	4.55	4.53	4.54	1.37	2.27	
55.73......	*Mn* II	4.69P	4.74P	5.20P	5.25P	....	0.75	5.37	1, 2
58.12......	*Ti* I	5.38p	5.11	5.16	5.38p	5.47P	9.64	2.24	
59.27......	*Ti* I	5.34p	5.19	5.16	5.60p	5.64P	9.69	2.25	
66.43......	*Mn* I	4.52p	4.49P	4.63p	4.60	4.58	1.23	2.91	
70.00......	*C* I	5.05p	5.36p	5.02p	4.98p	4.87	0.08	7.45	1
79.99......	*Ti* II	4.53	4.40	4.61	4.60	4.15	1.20	2.04	
83.42......	*Mn* I	4.44p	4.39	4.53	4.49	4.10	1.52	2.29	
4805.10......	*Ti* II	4.39	4.25	4.43	4.46	4.15	1.75	2.05	
10.53......	*Zn* I	4.43	4.40	4.68	4.68	4.63	1.56	4.06	
12.35......	*Cr* II	4.54	4.48p	4.81	4.75P	4.51	1.16	3.85	
23.52......	*Mn* I	4.37p	4.25	....	4.46	....	1.85	2.31	

NOTES TO TABLE 2

1. The line has very substantial contributions from other elements and is not used in all stars.
2. The solar strength is poor for various reasons. In most cases the strength in τ UMa was used for the analysis of the other F stars.
3. In the wing of a hydrogen line; not used in the curve of growth.
4. Almost certainly not *Si* II; strong in many F stars.
5. The only accessible *Eu* II lines are very badly blended.

earths, are needed. Such lines may be very weak in the sun, e.g., 5 mA, and may reach 50 mA in τ UMa. The blending effects of neutral and ionized elements in τ UMa also more closely resemble those in the A and F stars.

Accidental errors of the photometry are small. From the two independent tracings and reductions of the same plate of θ UMa it was found that the average difference (without regard to sign) was about 5 per cent of the equivalent width for good lines. Thus the total error of the microphotometer, of the drawing of the continuum and the line,

TABLE 3

EQUIVALENT WIDTHS, IN ANGSTROMS, OF LINES MEASURED ON OTHER SPECTROGRAMS

Star	Type	Source	$H\gamma$	$H\delta$	$H\zeta$	$H\eta$	$H\theta$	K
α Lyr	A0 V	CQ	21.4(4)	19.6(4)	14.5(4)	11.1(3)	8.6(3)	0.80(4)
		At	21.5	19.8	....	....	....	....
α CMa	A1 V	At	17.0	16.2	....	....	....	0.71
		Al	16.4	17.2	....	....	....	....
γ Gem	A1 V	Al	15.0(2)	14.4(2)	....	....	....	1.05(2)
η Oph	A2 V	CQ	17.5(2)	14.9(2)	12.8(2)	9.7(2)	7.5(2)	2.22(2)
κ Tau	A5 V	CQ	17.5(2)	17.4(2)	10.3(2)	8.8(2)	6.1(2)	4.15(2)
α Car	F0 II	Cd	8.7(2)	8.0(2)	....	....	....	4.9(2)
σ Boo	F2 V	CQ	7.4(3:)	6.7(3:)	5.7(3)	5.8(3)	4.1(3)	5.9(3)
		Hy	....	6.3	....	....	....	4.4
α CMi	F5 IV	At	7.7	7.4	....	....	....	....
		Hy	....	4.4	....	....	....	6.3
α Per	F5 I*b*	At	8.2	6.3	....	....	....	....
		Hy	....	....	....	....	....	7.6
ρ Pup	F6 II	CQ	6.6(2)	4.9	....	....	....	7.1(4)
		Cd	8.4(2)	8.4(2)	....	....	....	....
		Br	....	....	....	....	....	5.5
θ UMa	F6 III	CQ	....	....	....	....	....	8.7(1:)
		Cd	5.6	4.6	....	....	....	....
		Hy	....	1.8	....	....	....	6.7
		Br	....	....	....	....	....	7.5
τ UMa	A+F	CQ	11.1(3)	9.3(3)	7.6(3)	7.1(3)	4.9(3:)	3.39(3)
		Cd	11.0(3)	9.4(2)	....	....	....	....
		Br	....	....	....	....	....	2.8
15 UMa	A+F	CQ	11.4(3:)	8.2(3:)	7.3(3:)	7.2(2)	5.6(2)	3.19(3:)
ζ Lyr A	A+F	CQ	17.1(3)	17.4(3)	10.8(3)	8.5(3)	7.0(3:)	3.83(3)

and of the measurement and reduction is about 3 per cent per plate. A larger error arises from the systematic plate-calibration error. For 60 good lines measured on three different plates of τ UMa, the average deviation of an observation from the mean was 4.7 per cent for strong lines, 5.3 per cent for average, and 7.9 per cent for weak lines. After correction for the errors of measurement we find 5.5 per cent error per plate arising from plate calibration. (Of course, the entire calibration system may be wrong by a large amount, but no evidence for large systematic errors has yet been found.) In stars like θ UMa, α CMi, and α Per, where a single plate was used, a systematic error of about 6 per cent of the equivalent widths is possible, corresponding to ± 0.03 in log W/λ. A systematic error enters nearly linearly into the final value of the turbulent velocity derived and in a larger degree into the opacity, pressure, and surface gravity. These quantities are less well determined than the other deduced parameters, such as the level of ionization and the relative abundance of the elements.

Certain lines could not be satisfactorily measured on the present coudé plates. Table 3 contains results of my measurements of the hydrogen lines and the K line of *Ca* II on coudé and on other types of plates. The 500-mm camera, with two quartz prisms and Eastman Process plates, was used for the CQ series; hydrogen lines were also measured in the *Photometric Atlas*[2] ("At"), on my own coudé plates ("Cd"), and by Aller[5] ("Al"). Some new measures of relatively low weight were made on Yerkes Bruce plates ("Br"), and some were available by Hynek[6] ("Hy"). In parentheses I give the number of plates used. On short dispersion many metallic lines are included in the measured width of the hydrogen lines; the coudé tracings are also unsuitable for such measurements, since the hydrogen lines are about 6 feet wide. On the whole, the data in Table 3 must be considered of rather low weight. Table 3 also contains measures on certain standard A and F stars and on two other "metallic-line A stars," 15 UMa and ζ Lyr A.

LINE CONTOURS

The dispersion is sufficiently high to permit a study of the contours of strong lines; for moderate lines the instrumental contour requires investigation. Only in α Per is the turbulence large enough to permit a direct estimate of the Doppler broadening; even in this star a special investigation will be required on more suitable fine-grained plates. The apparent line widths decrease in the order α Per, ρ Pup, τ UMa, θ UMa, α CMi, which proves to be the order of decreasing turbulence. The stars are thus nearly free of rotation. Some general considerations on the central intensities may be of interest. In a preliminary analysis let us consider that the instrumental and the true line profile are both of Gaussian form. Let the true absorption, A, at a distance, x, from the center of the true line be

$$A(x) = A(0)\, e^{-(x/\alpha)^2} . \tag{1}$$

Let the instrumental contour be

$$K(x) = \frac{1}{\beta\sqrt{\pi}}\, e^{-(x/\beta)^2} . \tag{2}$$

The observed contour, $A'(x)$ will be

$$A'(x) = \frac{A(0)\,\alpha}{(\alpha^2+\beta^2)^{1/2}}\, e^{-(x/\alpha^2+\beta^2)} . \tag{3}$$

The equivalent width is

$$W = \sqrt{\pi}\,\alpha A(0) . \tag{4}$$

In an investigation[7] of α Car I found that β was of the order of 100 mA; the Doppler broadening and the strength of the line determine α. For very weak lines $\alpha \approx \Delta\lambda_D$, the Doppler width, and ranges from 100 mA to 20 mA for velocities of 10 and 2 km/sec. Now consider lines of equal equivalent width in two stars which have different Doppler broadening, α_1 and α_2. The true central absorptions will be

$$\frac{A(0, 1)}{A(0, 2)} = \frac{\alpha_2}{\alpha_1} . \tag{5}$$

The observed central absorptions will be

$$\frac{A'(0, 1)}{A'(0, 2)} = \left(\frac{\alpha_2^2+\beta_2^2}{\alpha_1^2+\beta_1^2}\right)^{1/2} . \tag{6}$$

The effect of Doppler broadening is to make the lines shallower; in stars of very large turbulence, like α Per or ϵ Aur, weak lines will eventually disappear because of low cen-

[5] *Ap. J.*, **96**, 321, 1942. [6] *Ap. J.*, **82**, 338, 1935. [7] *Ap. J.*, **95**, 161, 1942.

tral absorption and increased blending. For example, assume $\beta = 100$ mA, $\alpha_1 = 100$ mA, and $\alpha_2 = 20$ mA; then the apparent central absorption $A'(0, 1) = 0.7\ A'(0, 2)$, by equation (6).

In all F stars investigated, the apparent central absorption for strong lines (including the hydrogen lines) approaches 0.86. This is also true for τ UMa, the "metallic-line A star." One hypothesis to account for the apparently composite spectrum of τ UMa is that it is an unresolved binary, consisting of an F star and an A star. In such a binary we should expect to observe a central absorption, $A''(0)$ in a line of the F star given by

$$A''(0) = \frac{A(0, F) L(F)}{L(F) + L(A)}, \tag{7}$$

if $L(F)$ and $L(A)$ are the luminosities of the F and the A stars at the given wave length. Since $A''(0)$ (without correction for instrumental blurring) is 0.86, $1.00 > A(0, F) > 0.86$. From (7) we derive $L(A)/L(F) < 0.16$. Consider the superposition of an A-star spectrum in which the K line is absent on an F-star spectrum in which it has equivalent width $W(K)$. The apparent equivalent width in the composite spectrum would be

$$W''(K) = \frac{W(K) L(F)}{L(F) + L(A)}, \tag{8}$$

which involves a maximum possible reduction of less than 14 per cent of $W(K)$. According to Table 3, the K line in τ UMa is about 50 per cent as strong as in a normal F6 star. We may then conclude that no superposition of two spectra can be responsible for the metallic-line A-star spectrum.

Plotting the observed central absorption, $A'(0)$, against equivalent width in several stars gave the statistical relation between $A'(0)$ and W. No significant difference exists for these relations in α CMi and in τ UMa; since the former was measured on direct-intensity tracings[2] made at the University of Michigan and the latter on the Yerkes transmission microphotometer, the agreement shows that the photometric reductions are consistent in scale. For example, the values of W at which $A'(0) = 0.50$ are given in the accompanying tabulation in various wave-length regions. Note that the increase

	λ 4050	λ 4250	λ 4550
α CMi.	115 mA	133 mA	146 mA
τ UMa.	115	131	171

in W required to obtain $A'(0) = 0.50$ arises mainly from the prismatic dispersion; in fact, if we express the absorption in equivalent millimeters, the required W actually decreases about 20 per cent from λ 4050 to λ 4550.

The hydrogen-line contours are almost unaffected by the instrumental contour, except for scattered light. The extreme wings are easily lost when the continuum is drawn in. Smoothed contours for $H\gamma$ and $H\delta$ in the F stars are given in Table 4. The most striking feature is their similarity, over a range of 8 mag. in absolute luminosity; only small differences of $A'(0)$ or W exist between α CMi and α Per. The observational accuracy is not high, but a similar comparison at type A0 would show differences in W by a factor of 5. It is known that the strong negative luminosity effect in the A stars arises from the decrease of Stark broadening. On the other hand, in giant G and K stars the hydrogen lines are observed to be strengthened. Thus a null-effect in the F stars is not unexpected; more observational data on the hydrogen lines in F, G, and K stars is needed to explore these effects. We shall see in the last section of this paper that the strength of the hydrogen lines and the existence of extended wings in supergiant F stars is in accordance with theoretical expectation. The star τ UMa has stronger hydrogen lines than is normal for an F star but weaker than a normal A star. The star θ UMa has weak metallic lines and has the weakest hydrogen lines as well. Although he has not given a complete theoretical explanation, we may note that Hynek[6] has shown that some late F and G giants and subgiants have weaker lines than either dwarfs or supergiants have.

THE THEORY OF CURVES OF GROWTH

Theoretical methods for the analysis of the chemical constitution of stellar atmospheres can be divided into two main types. One involves the construction of a curve of growth for the star; since laboratory or theoretical intensities are lacking for most

TABLE 4

SMOOTHED HYDROGEN-LINE CONTOURS
$A'(0)$ IN PERCENTAGES

$\delta\lambda$	$H\gamma$					$H\delta$				
	τ UMa	α Per	ρ Pup	θ UMa	α CMi	τ UMa	α Per	ρ Pup	θ UMa	α CMi
0.0 Å	87	89	85	86	87	85	87	81	86	89
0.5	68	79	71	58	67	67	69	67	53	74
1.0	57	68	56	44	54	58	58	55	41	60
1.5	52	58	48	37	45	52	50	49	37	50
2	49	53	45	32	42	48	44	45	31	45
3	43	45	38	28	34	42	36	40	24	37
4	38	40	32	24	30	38	29	33	18	29
5	34	35	29	20	26	32	24	30	15	26
6	30	31	26	17	24	29	20	27	12	22
8	24	24	20	13	18	22	14	22	9	16
10	19	20	14	10	16	17	8	18	6	11
12	17	15	12	8	12	13	3	15	4	7
15	12	9	8	5	8	10	0	10	2	2
20	8	0	3	1	1	5	0	3	0	0
25	5	0	1	0	0	1	0	0	0	0
30	2	0	0	0	0	0	0	0	0	0
35	1	0	0	0	0	0	0	0	0	0

metallic lines, a curve of growth of the sun is used to determine semiempirical line intensities for the metallic lines. Another approach is taken in the analysis of the sun by Bengt Strömgren,[8] who obtains a detailed model giving the temperature, pressure, and opacity as a function of optical depth. For those few lines for which laboratory or theoretical f-values and damping constants are known, he computes rigorously the expected line contour and equivalent width for various abundances of the element and of the metals compared to hydrogen. This latter exact approach involves a knowledge of the physical parameters of the star—effective surface gravity and temperature. Since we are interested in many elements which lack f-values and since the gravity and temperature of most of our stars are unknown, we proceed by using a curve of growth. The availability of the exact theory, however, permits us to criticize and partially justify many of the assumptions of the theory of curves of growth.

Chandrasekhar[9] has recently obtained an exact solution for the absorption A_ν in a line as a function of η_ν, the ratio of the line-scattering coefficient to the continuous-

[8] *Pub. Kobenhavns Observatorium*, No. 127, 1940.

[9] *Ap. J.*, **106**, 147, 1947 (Paper XX).

absorption coefficient. The results are valid for the case in which the line is produced in an atmosphere where η is independent of optical depth, τ:

$$\lambda_\nu = \frac{\kappa_\nu}{s_\nu + \kappa_\nu}, \tag{9}$$

$$A_\nu = 1 - \frac{\lambda_\nu^{3/2}}{\frac{1}{3} + \frac{1}{2}\frac{B^{(0)}}{B^{(1)}}}\left(\alpha_2 + \frac{B^{(0)}}{B^{(1)}}\frac{\alpha_1}{\lambda_\nu} + \frac{1-\lambda_\nu}{2\lambda_\nu^{1/2}}\alpha_1^2\right). \tag{10}$$

The first and second moments, α_1 and α_2, of certain H-functions are tabulated for a set of values of λ. The constants $B^{(0)}$ and $B^{(1)}$ measure the limb darkening; in the usual linear approximation for the temperature as a function of τ,

$$\frac{B^{(0)}}{B^{(1)}} = \frac{8}{3}\frac{kT_0}{h\nu}\frac{\kappa_\nu}{\bar{\kappa}}. \tag{11}$$

Since we plan to use a single curve of growth for all frequencies, we must chose $B^{(0)}/B^{(1)}$ constant; its value is near 0.39 $\kappa_\nu/\bar{\kappa}$ for the sun. To compare with other computed curves of growth, e.g., Strömgren's,[8] we actually adopt $B^{(0)}/B^{(1)} = \frac{2}{3}$, corresponding to the latter's value:

$$\frac{x_0}{n} = \frac{h\nu}{kT_0}\frac{\bar{\kappa}}{\kappa_\nu} = 4 .$$

A value of x_0/n near 8 might be preferable, since $\kappa_\nu/\bar{\kappa}$ is near 0.7 for the sun. On the assumptions that η is independent of depth and that the line is formed by scattering, Strömgren obtains

$$A_\nu = \frac{1-\lambda}{1+\frac{2}{3}\sqrt{3\lambda}}. \tag{12}$$

A comparison of the values of A_ν computed according to these two Milne-Eddington (M.E.) models, equations (10) and (12), is given in Table 5. The ratio in the sense of *Chandrasekhar* divided by *Strömgren*, is in the fifth column. For comparison I also give the value of A_ν for a Schuster-Schwarzschild (S.S.) model in the last column. The S.S. model gives

$$A_\nu = \frac{s_\nu}{1+s_\nu} \tag{13}$$

and differs in its asymptotic form as $s_\nu \to 0$. To permit a comparison I have adopted $\kappa_\nu = 0.4641$ in the S.S. model, so that $s_\nu = 0.4641\,\eta_\nu$. Then the S.S. model agrees with the Strömgren M.E. model both for small and for large s_ν. In spite of this forced agreement, the deviations reach 20 per cent and are very systematic in nature. We can then expect serious differences in the curves of growth between the S.S. model and the M.E. model. The same remarks are valid for those curves developed by Unsöld, who uses

$$A_\nu = \frac{A(0)\,s_\nu}{A(0)+s_\nu}. \tag{14}$$

The data in Table 5 could be used to compute a complete curve of growth on the exact M.E. theory. For the present I limit myself to an estimate of the errors produced by the use of equation (12). For very weak lines, with $\eta_0 < 1$, the line absorption is everywhere small, and the exact value of the equivalent width will be about 9 per cent larger than that given by Strömgren. For very strong lines, $\eta_0 \gg 1$, the line is saturated, and the two expressions agree; in the extreme wings $\eta_\nu < 1$, and a 9 per cent error appears. The equivalent width will be less than 9 per cent in error, of course—probably near 4 per cent. Since the errors vary from 9 per cent for weak lines to 4 per cent for strong, the shape of the curve of growth will be nearly correct. An error of 5 per cent is 0.02 in $\log_{10} W/\lambda$; on the flat part of the curve of growth, where $d \log W/d \log \eta_0$ is about 0.25, errors of 0.08 in $\log \eta_0$ may occur. The curve for the S.S. model is very different in shape, and, if the conventional formula in equation (13) had been used, the strength of weak lines would have been doubled. Consequently, the theoretical curves of growth used by Allen,[10] K. O. Wright,[11] Unsöld,[12] and J. G. Baker[13] in most recent investigations of the solar and stellar curves of growth will not agree with those computed on the exact theory with constant η. In particular, the damping constant is systematically increased by the use of the S.S. model.

TABLE 5

PREDICTED ABSORPTIONS, A_ν

λ_ν	η_ν	Chandrasekhar	Strömgren	Ratio	S.S.
1.0	0.000	0.0000	0.0000	*	0.0000
0.9	0.111	0.0519	0.0477	1.087	0.0464
0.8	0.250	0.1061	0.0984	1.078	0.1040
0.7	0.429	0.1631	0.1526	1.069	0.1659
0.6	0.667	0.2238	0.2112	1.060	0.2363
0.5	1.00	0.2890	0.2753	1.050	0.3170
0.4	1.50	0.3609	0.3468	1.041	0.4104
0.3	2.33	0.4420	0.4288	1.031	0.5199
0.2	4	0.5385	0.5276	1.021	0.6499
0.1	9	0.6660	0.6593	1.010	0.8068
0.05	19	0.7588	0.7550	1.005	0.8981
0.00	∞	1.0000	1.0000	1.000	1.0000

* Note that, as $\eta_\nu \rightarrow 0$, the first-order expansion is $A_\nu \approx 0.4641\eta_\nu$ in Strömgren's formula (12). In eq. (10) it is necessary to obtain asymptotic expansions of the moments α_1 and α_2. I have done this only approximately and find $A_\nu \approx 0.4910\eta_\nu$, so that this ratio is 1.058 as $\eta_\nu \rightarrow 0$. The expansion of eq. (10) is based on the values of α at $\lambda = 1.0$ and $\lambda = 0.9$, not on the exact expansion at $\lambda = 1.0$. The probable limiting value of the ratio is near 1.096.

For the present analysis we must decide whether, in fact, the M.E. model with constant η is to be preferred to the S.S. model, in which the lines are formed in a layer where the re-emission in the continuum can be neglected. If, in fact, η decreased very rapidly inward, the S.S. model might be preferable. Only a detailed model for each type of line in each star will justify a choice—and if such models were available, the use of curves of growth would become unnecessary. Since we compare an F star with the sun, we wish to estimate the order of magnitude of the error produced in the F star, as compared to the sun, by the approximation η = constant. At present, model atmospheres for the sun[8] and for a bright dwarf F star[14] ($\theta_0 = 0.8$, $\log g = 3.5$) have been published by Strömgren and his collaborators. These models give θ, $\log P_g$, $\log P_e$, and $\log \bar{\kappa}$ as a function of τ, at frequent intervals in τ. Let us assume that the ionization and excitation follow the formulae of Saha and Boltzmann, with equal excitation and ionization temperatures. Then, for any element in a given stage of excitation, the number of active

[10] *Mem. Commonwealth Solar Obs., Canberra*, No. 5, 1934; No. 6, 1938.

[11] *Ap. J.*, **99**, 249, 1944.

[12] *Physik der Sternatmosphären* (Berlin, 1938), Fig. 85 and p. 266.

[13] *Ap. J.*, **84**, 474, 1936.

[14] *Pub. Kobenhavns Observatorium*, No. 138, 1944.

atoms can be computed at each τ; if we know the f-value and the damping, we can compute η_ν and eventually the exact line profile by an integration over τ. I have neglected the increase of damping with depth and have computed the absorption produced by various atoms in the cases, $\eta = 0.1$, $\eta = 1.0$, and $\eta = 10$, at optical depth $\tau = 0.3$. The latter value is a useful representative point in the star; the range of values of η covers both weak and moderately strong lines. The line absorption was computed from

$$A = \frac{1 - \overline{\lambda}}{1 + \frac{2}{3}\sqrt{3}\ \overline{\sqrt{\lambda}}}, \tag{15}$$

where $\overline{\lambda}$ and $\overline{\sqrt{\lambda}}$ are properly weighted averages of λ and $\sqrt{\lambda}$ in the atmosphere. The method of averaging, using a five-point Gaussian division, follows that given by Strömgren.[15] Unfortunately, if λ varies with τ, the points in the atmosphere λ_0, about which the Gaussian division should be taken, should be determined so as to give the most accurate representation. This problem requires further exploration. If we arbitrarily take λ_0 to be the value at the boundary of the star, say at $\tau = 0.01$, we heavily weight the outer layers of the star. This representative point is best for very strong lines and undoubtedly exaggerates the effect of the variation of λ with τ for normal lines. Except in the most luminous stars, broadening of lines by collisions either with electrons or with hydrogen atoms produces an effective increase of η with depth in the wings of a line. Since most of the decrease of η normally arises from the increase of κ_ν, which is proportional to P_e, pressure-broadening tends to make η independent of depth and further reduces the effects revealed in the model that we have adopted.

Typical atoms listed in Table 6 in various states of excitation were chosen. I computed, with $x_0/n = 4$, the absorptions, $A(F)$ in the F star and $A(\odot)$ in the sun. The table also gives $A(\eta)$, from equation (12), computed on the assumption of $\eta =$ constant, and A(S.S.) according to equation (13). The variations of η are quite large; in the F star, η for metallic lines decreases by a factor of 10 from $\tau = 0.05$ to $\tau = 1.0$, and for the hydrogen lines shows a slow increase. In the sun the resonance *Fe* I, *Fe* II, and *Ca* II lines show larger decreases; the excited *Fe* II lines have constant η, and the hydrogen lines have η increasing by twenty times in the same range. Since Table 6 neglects the pressure dependence of η and overweights the upper layers, it gives line absorptions that lie rather close to the S.S. values. Nevertheless, if we compare the F stars and the sun, we find in the main that the differences are small, i.e., that if two lines have the same η at a representative point in an F star and in the sun, the line absorption will be similar. Variations are of the order of 10 per cent, except for the wings of the hydrogen lines, which are produced at great depths in the sun. (The pressure-dependent Stark broadening will further increase the latter effect.)

A preliminary test was made of the effect of weighting less strongly the upper layers of the atmosphere. For large η this will introduce only small changes in Table 6, since such lines are formed at small τ. However, for $\eta = 1.0$, I chose λ_0 to be the value of λ at $\tau = 0.3$ and made the Gaussian summations about that value of λ_0. The results for the *Fe* II line at 0 volts were $A(F) = 0.293$, $A(\odot) = 0.295$; for the hydrogen lines, $A(F) = 0.288$, $A(\odot) = 0.284$. These absorptions lie close to the value for $\eta =$ constant, i.e., $A = 0.275$, and show little change from star to star. We may take this evidence and the data in Table 6 as a first attempt to justify the use of curves of growth. In the main the effects of stratification cancel out when we compare the F stars and the sun. Over wider ranges of temperature and pressure this cancellation may not occur. Comparing dissimilar lines in the same star leaves a larger effect. Since changes of the order of 25 per cent occur between the predicted absorptions for different elements in different stages of excitation, similar systematic changes of equivalent width may occur. It is possible that the abnor-

[15] *Ibid.*, No. 127, p. 243, 1940.

mally low excitation temperature indicated in all stars by metallic lines of low excitation potential is connected with the systematic weakness of the excited lines in Table 6. The low opacity of the outer layers produces a rapid decrease of η with increasing depth; at low excitation potential the large boundary value of η gives very strong absorption lines, while for highly excited lines, η may be constant, and the line will be relatively weakened. Lines of high excitation potential may be strengthened by stratification especially if subject to pressure broadening. Different curves of growth for different elements and deviations from a simple theoretical curve of growth may also be expected.

In the actual analysis a set of curves of growth based on the M.E. model with constant η was available from the computations of Pannekoek and van Albada.[16] They have shown that their curves agree within 0.01 in log W with that given by Strömgren. They give the equivalent width in units of the Doppler width, $(A/2b)$, as a function of log s_0/κ (our log η_0) for various values of the ratio, a, of the damping to the Doppler

TABLE 6

COMPARISON OF ACTUAL LINE INTENSITIES IN MODEL ATMOSPHERES AND THE PREDICTED ABSORPTIONS WITH η CONSTANT

ELEMENT	E.P. (VOLTS)	$\eta=0.1$		$\eta=1.0$		$\eta=10.0$	
		$A(F)$	$A(\odot)$	$A(F)$	$A(\odot)$	$A(F)$	$A(\odot)$
Fe II	0	0.055	0.050	0.38	0.35	0.82	0.78
Fe II	3	.048	.049	.34	.31	.78	.72
Fe I	0	.047	.047	.32	.34	.78	.80
Fe I	2	.042	.041	.30	.31	.76	.76
Ca II	0	.059	.049	.39	.32	.83	.78
H I	10	0.050	0.105	0.29	0.30	0.67	0.60
$A(\eta)$		0.043		0.275		0.674	
A(S.S.)		0.044		0.316		0.823	

width. To transform to the notation most used recently, we proceed as follows: The observed curves of growth, in which log W/λ is plotted against log X_f, are slid both horizontally and vertically until a best fit with the theoretical curve is obtained. From these shifts and the value of a, we derive

$$\log\frac{W}{\lambda}-\log\frac{A}{2b}\equiv\Delta\log\frac{W}{\lambda}\,, \tag{16}$$

$$\log\frac{s_0}{\kappa}-\log X_f\equiv\Delta\log X_f\,, \tag{17}$$

$$\log V=\Delta\log\frac{W}{\lambda}+10.18\,, \tag{18}$$

$$\log\eta_0=\log X_f+\Delta\log X_f\,, \tag{19}$$

$$\log\frac{\Gamma}{\gamma_{cl}}=\log aV-2.92\,. \tag{20}$$

[16] *Pub. Astr. Inst. Amsterdam*, No. 6, 1946.

The velocity parameter, V, is

$$V = c \frac{\Delta\lambda_D}{\lambda} \tag{21}$$

and can be converted into a root-mean-square velocity by multiplication by $\sqrt{3/2}$.

THE OBSERVED CURVES OF GROWTH

The homogeneous nature of the observational data in Table 2 provides an opportunity for a systematic study. However, the interpretation must be based on several assumptions and approximations. We must attempt to derive information as to the physical conditions in the stars and as to the abundances of the elements by indirect means. We assume that the radiative transfer in subordinate lines follows the general lines of that within a resonance line. The distribution of atoms in the excited levels is supposed to follow a Boltzmann formula, with a unique excitation temperature, T_{exc}. The ionization of all elements is supposed to follow a Saha formula, without reference to the detailed ionization and recombination processes, at a single ionization temperature, T_{ion}, and electron pressure, P_e. The ratio of s_ν/κ_ν is taken as independent of optical depth. If turbulence exists, we assume that all atoms possess the same mean peculiar motion, described by a Gaussian distribution with velocity V. We must also permit the effective value of the surface gravity, g_e, of a star to differ from the gravitational value g.

With these assumptions we can proceed to compare the F stars to the sun. Based on the accurate solar intensities of Allen[10] and the Utrecht *Atlas*,[17] many solar curves of growth have been prepared, with either theoretical or laboratory intensities. In the analysis of the sun by K. O. Wright,[11] laboratory intensities are used to obtain a curve-of-growth relation between W and laboratory intensity, log X_f (with arbitrary zero point). Once this curve is established, semiempirical values of log X_f for all solar lines can be obtained. There is a systematic difference between the best-observed solar curve and the theoretical curve based on the S.S. model fitted to it by Wright. He found[11] residuals of about ± 0.17 in log X_f. Unfortunately, a re-analysis with the theoretical curves of the M.E. model does not improve these residuals appreciably. The shape of the observed curve differs from that of either theoretical type.[17a] One important factor may be the omission of the variation of κ_ν over the wave-length range covered by the solar observations; this same omission may partly explain the low solar excitation temperature. A trial fit of Wright's observed curve of growth with the M.E. curves gives

$$\log V = 5.34 \pm 0.04 \;,$$

$$\log a = -1.8 \;,$$

$$\frac{\Gamma}{\gamma_{cl}} = 4.3 \pm 0.5 \;,$$

$$\log \eta_0 = \log X_f + 2.14 \;.$$

K. O. Wright found $\Gamma/\nu = 2.61 \times 10^{-6}$, which corresponds to $\Gamma/\gamma_{\text{cl}} = 15$. Our new solar damping constant is only one-third the old. Since it has been pointed out for some time that most stars had apparently excessively large damping constants, this reduction is important. A re-analysis of my curve of growth for α Car,[7] which had $\Gamma/\gamma_{\text{cl}} = 10$ when interpreted with Baker's S.S.-type curves of growth,[13] gives a corrected value of

[17] Minnaert, Mulders, and Houtgast, *Photometric Atlas of the Solar Spectrum* (Utrecht, 1940).

[17a] *Note added in proof:* A redetermination of the solar curve of growth by Pierce and Goldberg (*Quarterly Progress Report, ONR Project M720-5* [Ann Arbor, October, 1947]) results in slightly smaller residuals when a M.E. model is used and when the variation of κ_ν is taken into account. Large discrepancies persist in the damping portion of the curve.

$\Gamma/\gamma_{cl} = 5$. All the F stars in this investigation prove to have nearly the classical damping constant. It is worth noting that the collisional damping for λ 3933 of *Ca* II has been derived by Strömgren for the sun.[8] From quantum-mechanical computations the damping is found and is proportional to the total gas pressure; if we evaluate it at a representative point, $\tau_0 = 0.3$, where $\log P_g = +4.80$, we find $\log a = -1.8$, in perfect agreement with the statistically determined value of $\log a$ given above for the neutral metallic lines in the sun. We have not justified in detail the use of a constant value of η for neutral subordinate lines in the sun or in the F stars. However, it is probably still to be preferred to the S.S. model, which corresponds to $\eta = 0$ except at the boundary.

The analysis of the stellar-line intensities proceeded in the conventional manner. The stellar values of $\log X_f$ for a line of excitation potential, χ, were computed for different excitation temperatures from

$$\log X_f'' = \log X_f + 5040\chi \left[\frac{1}{T(\odot)} - \frac{1}{T(*)}\right]. \tag{22}$$

The excitation temperature for the *Fe* I lines was determined by trial and error. Wright's value of $T(\odot) = 4850°$ was adopted for *Fe* I, and it was assumed that in the star all elements had the same excitation temperature. For most ions only partial curves of growth could be prepared. These were shifted horizontally to obtain a fit with the *Fe* I curve; a composite curve of growth for the ions and the neutral elements, excluding *Fe* I, was thus obtained. It was found that in all cases the theoretical curve determined for *Fe* I represented equally well the observed curve for *Fe* I and the composite curve for the other elements. From the measured intensity in the star $\log X_{f,i}''(*)$ was read for each line from the stellar curve of growth. Then the mean shift was determined for element i from

$$S_i = \overline{\log \frac{X_{f,i}''(*)}{X_{f,i}''(\odot)}}. \tag{23}$$

For each star a scale correction, δ, to the $\log X_f''$ of *Fe* I is required, because of the changing abundance of *Fe* I. Define

$$\delta \equiv \log \eta_0 - \log X_f''. \tag{24}$$

The value of $\delta(\odot)$ proves to be $+2.14$; for each other atom or ion,

$$\overline{\log \frac{\eta_{0,i}(*)}{\eta_{0,i}(\odot)}} = S_i + \delta(*) - \delta(\odot). \tag{25}$$

From the definition of η_0, we find

$$\Delta \log \zeta_i(*) \equiv \log \frac{\dfrac{N_i(*)}{\kappa_\nu(*)}}{\dfrac{N_i(\odot)}{\kappa_\nu(\odot)}} = \log \frac{\eta_{0,i}(*)}{\eta_{0,i}(\odot)} + \log \frac{V(*)}{V(\odot)}, \tag{26}$$

where $\Delta \log \zeta_i(*)$ may be considered the apparent relative abundance of the given atom in the star as compared to the sun; it is analogous to (N_iH) in the S.S. type of analysis, the number of atoms above a square centimeter of the photosphere. From equation (26) we determine the relative number of atoms of a given ion per gram of stellar material, in units of the continuous absorption coefficient per gram. In this discussion we shall neglect the small variation of κ_ν over the 750-A range covered.

We may wish to use a value of η_0 in a given star, as predicted from its value in the star τ UMa, for which the observational accuracy was greatest. Since we shall have tabulated the values of $\Delta \log \zeta_i$ in various stars, we use the relation

$$\log \eta_0(*) = \log \eta_0(\tau) + \Delta \log \zeta_i(*) - \Delta \log \zeta_i(\tau) - \log \frac{V(*)}{V(\tau)}. \quad (27)$$

In the sun we read $\log X_f$ from the *observed* curve, while in τ UMa we used the *theoretical* curve of growth. While there is an inconsistency in principle, in practice the stellar data cannot certainly establish a difference. We are thus now able to predict the intensity of a line in a star from its intensity both in τ UMa and in the sun. Different observational errors enter these two predictions; the blending effects in the F stars are in part eliminated by using measures in the same type of star, as observed with the same dispersion. The spectrum and probably the physical conditions in ρ Pup and α Per resemble τ UMa much more closely than they do the sun.

A systematic comparison of the values of $\log X_f''$ and $\log \eta_0(\tau)$ for different elements is of interest. Let us assume a linear relation:

$$\log \eta_0(\tau) = a + b \log X_f''. \quad (28)$$

We find that b is nearly unity for most elements, except that $b = 1.48$ for *Cr* II and $b \approx 1.4$ for strong lines of *Ti* II. The solar X_f'' are poor for *La* II and *Ce* II, which give $b \approx 0.6$. Thus *Cr* II, and *Ti* II slightly, may show different curves of growth in certain stars, when plotted against solar $\log X_f''$. Aller[18] pointed out what may be an extreme example of this phenomenon in α Cyg, where the curves of growth for *Cr* II and *Ti* II differed substantially from that for *Fe* II. In several of this group of F stars, the curve of growth for *Ti* II is definitely peculiar. There may be physical processes, such as stream motions or variations of η with depth, that actually alter the curves of growth of certain elements in the sun and the stars. The previously noted differences between the solar observed and theoretical curve of growth are also quite significant. Let us read from the new theoretical curve of growth of the sun the values of $\log \eta_0(\odot)$. Then, if we write

$$\log \eta_0(\odot) = \alpha + \beta \log X_f'', \quad (29)$$

we can choose ranges of $\log X_f''$ where β differs very substantially from unity. For $-1.5 < \log X_f'' < -0.5$, I find $\beta \approx 0.7$; for $-0.5 < \log X_f'' < +0.5$, $\beta \approx 1.0$; for $+0.5 < \log X_f'' < +1.5$, $\beta \approx 1.3$. In the mean, β is near unity.

The final results of the analysis of the various stars are collected in Table 7, which gives the values of $\Delta \log \zeta_i$ for 32 elements. The number of lines used is given in parentheses, with a colon (:) if the determination is poor. The table also contains parameters derived from the curve of growth, the excitation temperature ($\theta_{\text{exc}} = 5040/T_{\text{exc}}$), and the spectroscopically estimated absolute magnitude, M_s. Other tabulated quantities which will be discussed later are the absorption coefficient, κ_ν, at a mean wave length near 4300 A; the ionization temperature, θ_{ion}, the electron pressure, P_e, the total pressure, P_g, and the surface gravity, g_e and g. The quantities δ are defined in equation (24).

The curves of growth for τ UMa, ρ Pup, and θ UMa are shown in Figures 1–10; the curves for α Per and α CMi will be given in Paper II of this series. They are plotted against $\log X_f''$, the solar values corrected to the excitation temperature shown. The observational scatter is small; the *Fe* I curve has about 115 plotted points, of which only 10 lie more than ± 0.20 in $\log W$ off the theoretical curve in τ UMa (Fig. 1) and only 5 each in ρ Pup (Fig. 4) and θ UMa (Fig. 8). Most discrepant lines show appreciable blending. In Wright's curve of growth for the sun[11] about 5 per cent of the lines also

[18] *Ap. J.*, **95**, 73, 1942.

TABLE 7

UNCORRECTED RATIO OF APPARENT ABUNDANCES, F STAR TO SUN

$\Delta \log \zeta_i$

Element	τ UMa	ρ Pup	θ UMa	α CMi	α Per	Notes
C I	−0.4 (1:)	−0.5 (1:)	+0.3 (1:)	+0.2 (1:)	......	......
Mg I	−1.30 (5:)	−0.92 (5)	−0.45 (7)	−0.10 (5:)	−0.9 (4)	......
Mg II	$+1.9+a_1$ (3:)	$+2.3+a_1$ (3:)	$+2.5+a_1$ (3:)	$+2.2+a_1$ (2:)	$+2.6+a_1$ (1:)	1
S I	+0.25 (2)	+0.49 (3)	+0.25 (3)	+0.17 (3)	+0.48 (3)	......
Ca I	−1.49 (9)	−0.61 (10)	−0.25 (10)	−0.07 (8)	−0.59 (8)	......
Ca II	$-0.78+a_2$ (1:)	$-0.18+a_2$ (1:)	$-0.18+a_2$ (1:)	a_2 (1:)	$-0.1+a_2$ (1)	2
Sc II	−0.58 (8:)	+0.03 (10)	+0.35 (8)	+0.41 (8)	+0.5 (5)	......
Ti I	−0.74 (12)	−0.57 (10)	−0.14 (13)	−0.43 (8)	−0.57 (9)	......
Ti II	+0.47 (27)	+0.77 (26)	+0.54 (26)	+0.71 (25)	+0.96 (20:)	......
V I	−1.14 (5)	−1.02 (6)	−0.73 (6)	−0.93 (5)	−1.3 (3)	......
V II	+0.56 (4)	+0.63 (4:)	+0.03 (4:)	+0.7 (4)	+0.6 (3)	......
Cr I	−0.30 (10)	−0.30 (9)	−0.28 (10)	−0.23 (9)	−0.4 (5)	......
Cr II	+1.20 (9)	+0.88 (10)	+0.49 (9)	+0.57 (10)	+1.24 (8)	......
Mn I	−0.47 (12)	−0.67 (7)	−0.45 (7)	−0.18 (12)	−0.4 (8)	......
Mn II	a_3 (4:)	a_3 (6:)	$-0.2+a_3$ (5)	$-0.4+a_3$ (3:)	$+0.5+a_3$ (1:)	1, 3
Fe I	−0.60 (120)	−0.52 (115)	−0.43 (121)	−0.23 (117)	−0.63 (84)	......
Fe II	+1.20 (21)	+1.06 (22)	+0.56 (21)	+0.98 (20)	+1.37 (16)	......
Co I	−0.73 (4)	−0.88 (4)	−0.7 (3)	−0.5 (4:)	−1.0 (3)	......
Ni I	+0.18 (9)	+0.03 (8)	−0.08 (9)	−0.03 (9)	−0.41 (7)	......
Ni II	$+0.9+a_4$ (2)	$+0.50+a_4$ (3)	$+0.4+a_4$ (3)	$+0.2+a_4$ (3)	$+0.7+a_4$ (3)	4
Zn I	+0.35 (2)	+0.14 (2)	+0.05 (2)	0.0 (2)	−0.4 (2)	......
Sr II	+0.70 (3)	+0.85 (3)	−0.01 (3)	+0.49 (3)	+0.8 (2)	......
Y II	+0.99 (5:)	+1.07 (5)	+0.45 (5)	+0.55 (5)	+0.9 (1)	......
Zr II	+0.18 (7:)	+0.69 (6)	+0.15 (7)	+0.36 (7)	......	......
Ba II	+0.77 (2)	+0.55 (2)	+0.23 (2)	0.0 (2)	0.0 (1)	......
La II	+0.97 (10)	+0.73 (7)	+0.34 9)	+0.35 (9)	+0.9 (4:)	......
Ce II	+0.90 (8)	+0.58 (8)	+0.32 8)	+0.05 (8)	+0.8 (3)	......
Pr II	+1 0 (3)	+0.8 (3)	+0.4 (3:)	0.0 (2:)	......	5
Nd II	+1.1 (3)	+0.8 (3)	+0.5 (3:)	−0.1 (2:)	......	5
Sm II	+1.1 (4)	+0.9 (4:)	+0.5 (4)	+0.4 (3:)	......	5
Eu II	$+1.9+a_5$ (2:)	$+1.6+a_5$ (2:)	$+0.5+a_5$ (2)	$+0.8+a_5$ (2:)	$+1.2+a_5$ (2:)	5
Gd II	+0.9 (4)	+0.6 (4)	+0.4 (4:)	0.0 (4:)	+1.1 (1:)	5
$\delta(*)$	+1.28	+1.25	+1.61	+1.79	+1.06	......
$\log V$	+5.60	+5.70	+5.44	+5.46	+5.80	......
Γ/γ_{cl}	1.5	1.2	1.7	1.4	1.5	......
θ_{exc}	0.91	0.95	0.98	0.96	0.98	......
Spectrum	F6 II+A3	F6 II	F6 III	F5 IV	F5 I*b*	......
M_s	+3	−3	+1.5	+2.5	−5	......
$\log \kappa_\nu$	−1.62	−1.36	−1.00	−1.18	−1.64	......
θ_{ion}	0.86	0.83	0.87	0.86	0.82	......
$\log P_e$	0.0	+0.4	+0.6	+0.5	+0.1	......
$\log P_g$	+2.7	+3.0	+3.9	+3.6	+2.3	......
$\log g_e$	+1.6	+2.1	+3.4	+2.9	+1.2	......
$\log g$	+4.0	+2.5	+3.5	+3.7	+1.7	......

NOTES TO TABLE 7

1. The high excitation potential of *Mg* II and *Mn* II makes these determinations very uncertain. If there are departures from a simple Boltzmann distribution or if the scale of T_{exc} is incorrect, the comparison of F stars and the sun is difficult. Let the value of $\log \eta_0(\odot)$ require an arbitrary correction ($-a_1$ or $-a_3$); then the intercomparison of the F stars can proceed, subject to this zero-point correction.

2. The great strength of λ 3933 of *Ca* II, the only available line, makes this a very poor determination. The measured intensities are taken from different sources. In particular, the damping constant, which is the dominant quantity for strong lines, is poorly determined observationally in the F stars. Two values of $\log \eta_0(\odot)$ may be used, one based on the extrapolation of the observed curve of growth (+6.19) and the other on the theoretical curve (+6.82). The latter is exactly Strömgren's collisional-broadening value. If we write $\log \eta_0(\odot) = +6.82 - a_2$, we may later try to adjust a_2 for the normal F stars.

3. The identification of *Mn* II is very poor, and only Rowland intensities were available. The arbitrary zero point, a_3, will be set later.

4. A systematic difference between the results for *Ni* I and *Ni* II indicates that a zero-point correction to the solar strengths is required. Both *Ni* I and *Ni* II are at present somewhat unsatisfactory.

5. The rare earths are weak and badly blended in the sun, and Rowland intensities had to be used. Arbitrary zero-point corrections may be needed. In practice the line strengths in τ UMa, $\eta_0(\tau)$, were used to determine the relative abundances in the F stars. The latter comparison is accurate, and the uncertainty appears relative to the sun.

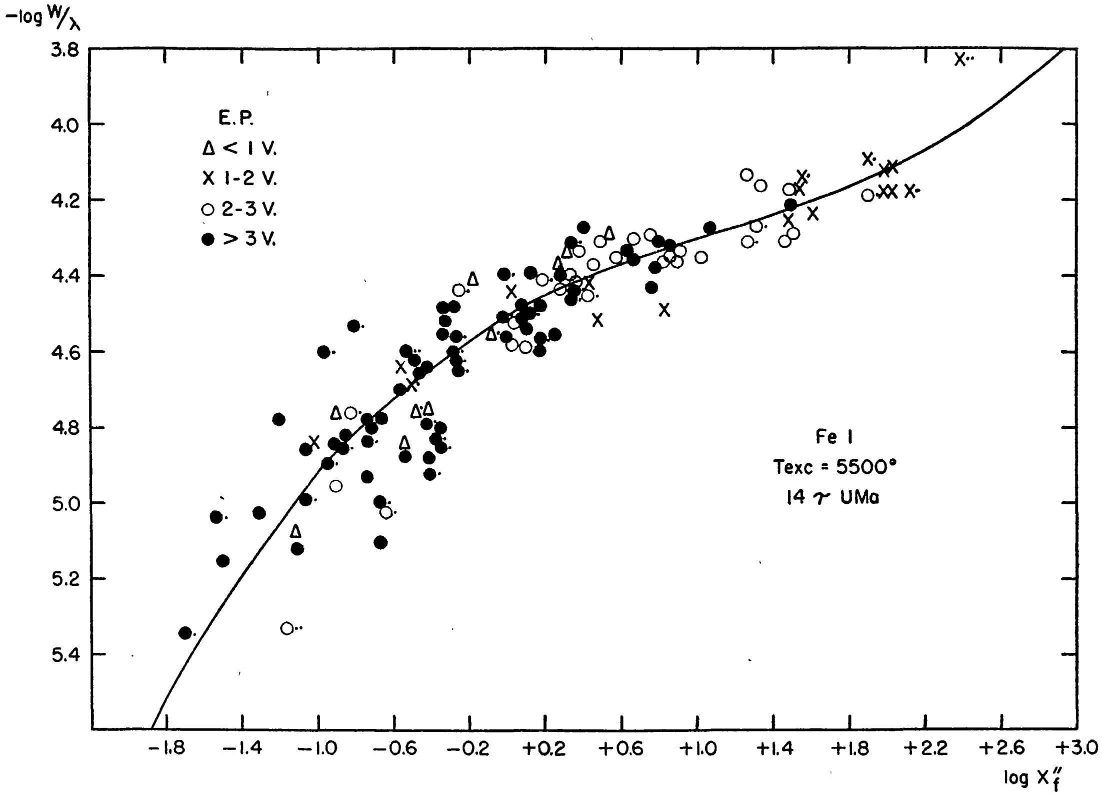

FIG. 1.—The curve of growth of *Fe* I for the metallic-line star, τ UMa. The abscissae are the line-absorption coefficients, X''_f based on the solar values of K. O. Wright. They are derived from the *observed* solar curve of growth, corrected to the excitation temperature of the star. The zero-point shift, δ(∗), is given in Table 7. The theoretical curve of growth is plotted.

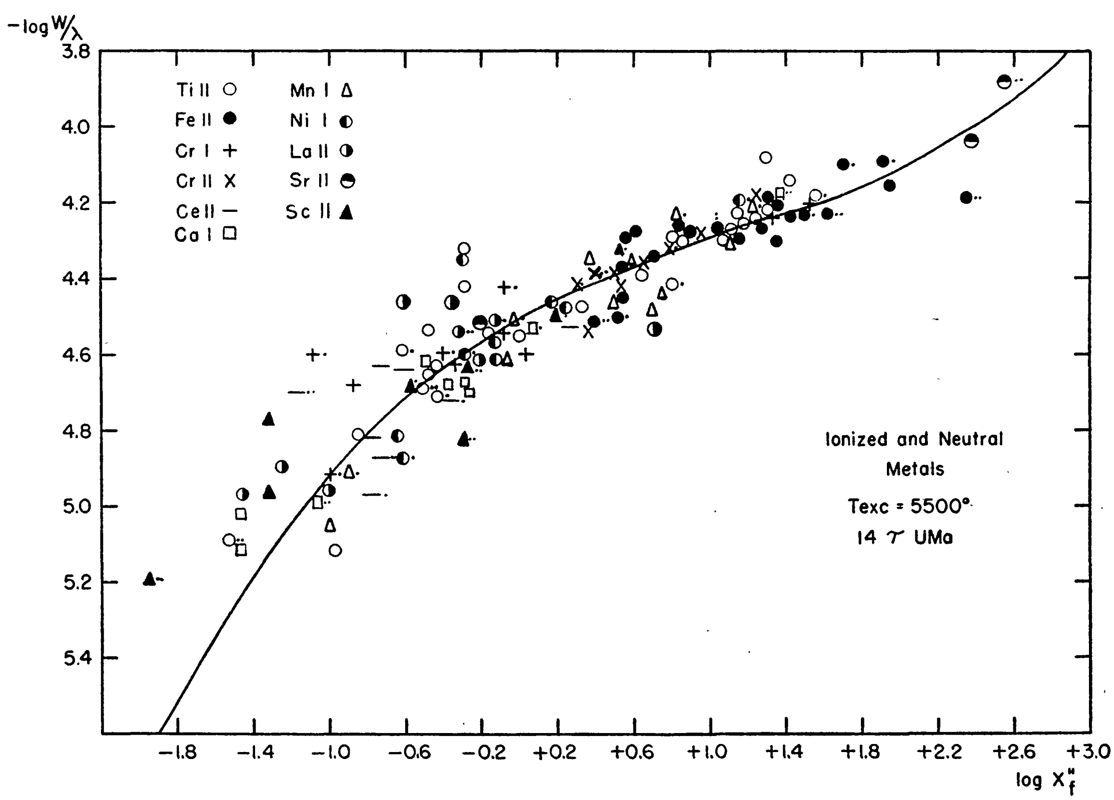

FIG. 2.—The curve of growth for other elements in τ UMa

deviate by ± 0.20 in log W. Since all solar errors reappear in the stellar curves, it seems probable that nearly all the residual scatter can be explained by errors in solar log X_f''-values and by the increased blending in the stars. The curves drawn are the theoretical curves, parameters of which are given in Table 7; the same theoretical curve is used in the plot for *Fe* I and for the other elements.

Figure 3 is a special curve for *Fe* I in τ UMa. Instead of using the solar log X_f'', based on Wright's *observed* solar curve of growth, I redetermined log η_0 ($\odot$), using the *theoretical* solar curve of growth. These η_0 ($\odot$) were corrected to the excitation temperature of τ UMa, giving the revised solar η_0' used in plotting Figure 3. The complicated residuals exemplified in equation (29) reappear in Figure 3 and result in a very peculiar diagram. (The plotted theoretical curve for τ UMa is the same as in Figs. 1 and 2.) The scale of log η_0' is compressed for lines that fall at the transition between Doppler and flat portions of the curve of growth of the star. It is enough expanded near the damping portion to require a damping less than the classical value. No theoretical curve would fit satisfactorily when the scale of log η_0' is used.

If we were to plot the curve of growth of τ UMa against the $\eta_0(\tau)$ given in Table 2, we should have zero residual scatter by the definition of $\eta_0(\tau)$. If we prepare curves of growth for ρ Pup and θ UMa, using $\eta_0(\tau)$ computed according to equation (27), we have a test of the quality of these $\eta_0(\tau)$. Figures 6, 7, and 10 present such curves of growth, together with the original *Fe* I theoretical curve derived for these stars. The residual scatter is considerably reduced in Figure 10, compared to Figure 9, for θ UMa. But the curves for *Fe* I (Fig. 6) and for the other elements (Fig. 7) in ρ Pup show, I believe, less scatter than any previously published curves of growth. No point deviates by ± 0.20 in log W, and only 10 per cent of the lines deviate by more than ± 0.10. Several elements have been omitted from Figures 7 and 10 because their Δ log $\zeta_*(*)$ were poorly determined. (In all these curves it should be remembered that a systematic positive residual in log W is to be expected for very weak lines; they will be absent on plates in which they are accidentally weak; blending also increases log W.)

The curves of growth seem quite normal, and no large systematic deviations are detected for any elements. The rare earths, *Ce* II and *La* II, fit the standard curve quite well, especially when $\eta_0(\tau)$ is used. Certain elements which are greatly weakened in τ UMa, like *Ca* I, *Sc* II, and *Zr* II, still fall on the standard curve. The poor solar X_f'' of *Cr* II and *Ti* II found in the discussion of equation (28) appear to have only small effect. Certain important lines are badly blended, even on this dispersion. The strongest *Fe* I line, λ 4045, is far off the curve, especially in τ UMa (Fig. 1). Examination of the line contour shows that what was measured as *Fe* I, λ 4045.82, actually included lines measured by Swensson[4] in α CMi at $\lambda\lambda$ 4045.39, 4045.64, 4046.01, 4046.42. In supergiant F stars, as λ 4045.82 widens, its intensity is increased very rapidly by such blending. (The great width of the turbulently broadened lines in supergiants probably has a different origin. Much recent work has indicated that line contours in supergiants may be very appreciably broader than those predicted from the turbulence given by the curve of growth.) Some of the excessive strength of λ 4077.71 of *Sr* II compared to λ 4215 has the same origin; the lines at $\lambda\lambda$ 4076.60, 4076.81, 4078.39, and especially λ 4077.35 of *La* II and λ 4077.94 of *Dy* II, blend with *Sr* II. In Figure 2 for τ UMa and Figure 5 for ρ Pup, the *Sr* II doublet deviates in slope from the theoretical curve. In Figure 7, however, where $\eta_0(\tau)$ was used in ρ Pup, the doublet falls close to the curve. These and other blending effects must be important for classification and luminosity criteria on low-dispersion spectra. The intensity of a badly blended line varies rapidly as the blending changes, and many strong features of low-dispersion spectral criteria are such blends. One example is the group of lines at λ 4172, λ 4178, important in F stars. They appear as a strong doublet in the Yerkes *Atlas of Stellar Spectra*;[1] in supergiant stars like ϵ Aur, α Per, and γ Cyg, the λ 4178 component is very strong. Both λ 4172 and λ 4178 contain many lines, but the λ 4172 blend has important neutral-line contributors, while λ 4178 is dominated

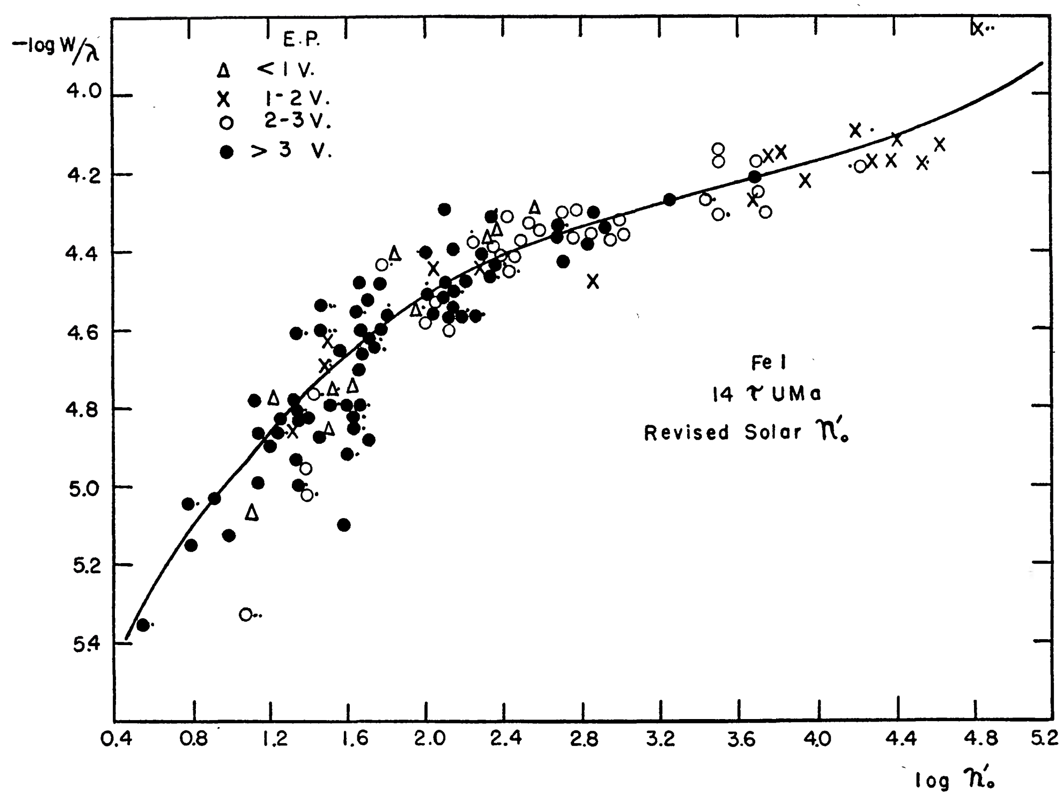

FIG. 3.—The curve of growth for *Fe* I in τ UMa, with the $\eta'_0(\odot)$ as abscissae; these are read from a *theoretical* curve of growth of the sun and are corrected to the excitation temperature of the star. Note the systematic nature of the residuals.

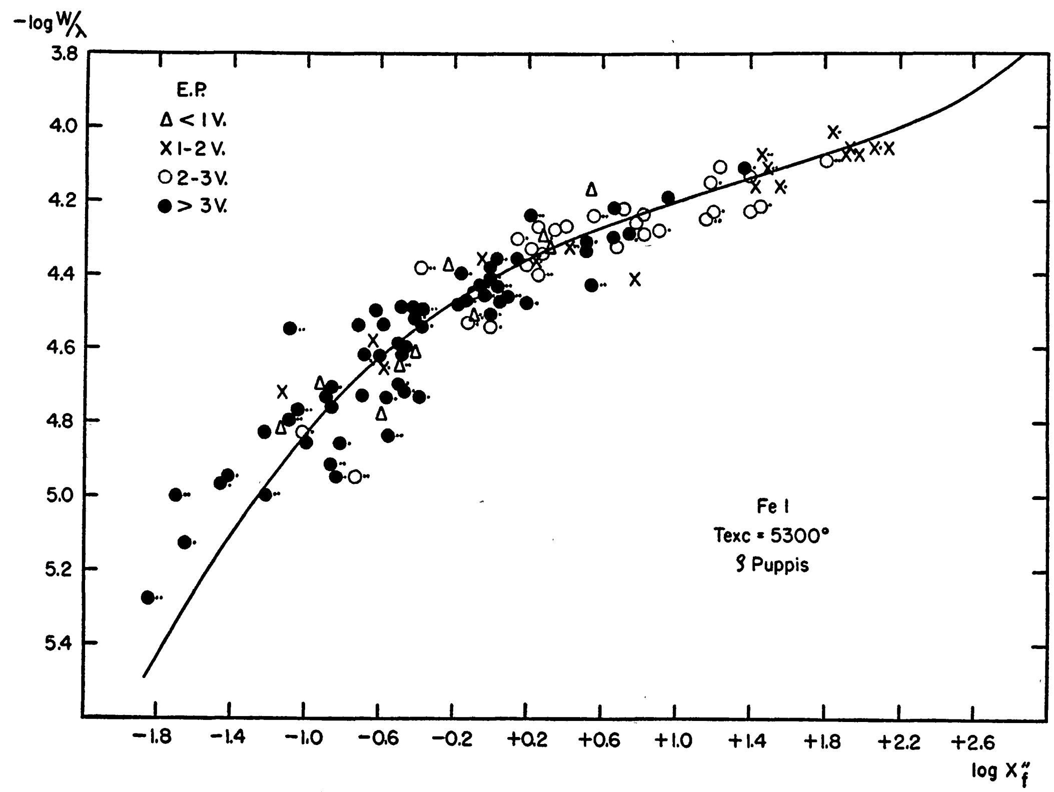

FIG. 4.—The curve of growth of *Fe* I in the supergiant ρ Pup, using solar X''_f

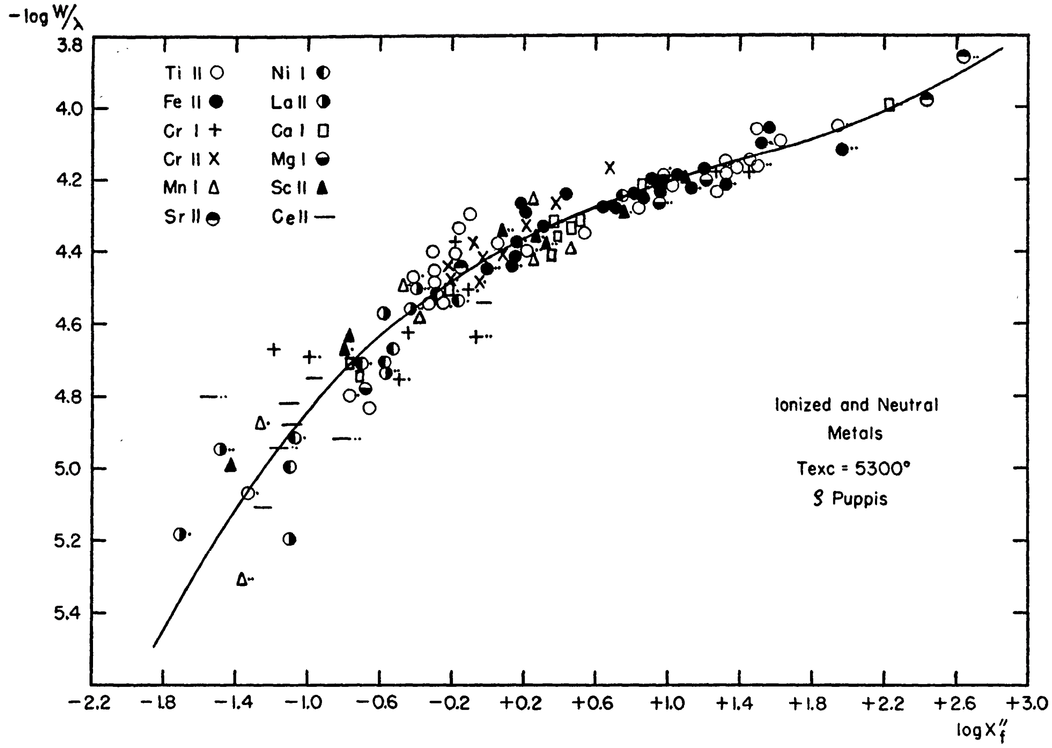

FIG. 5.—The curve of growth for other elements in ρ Pup, using solar X_f''

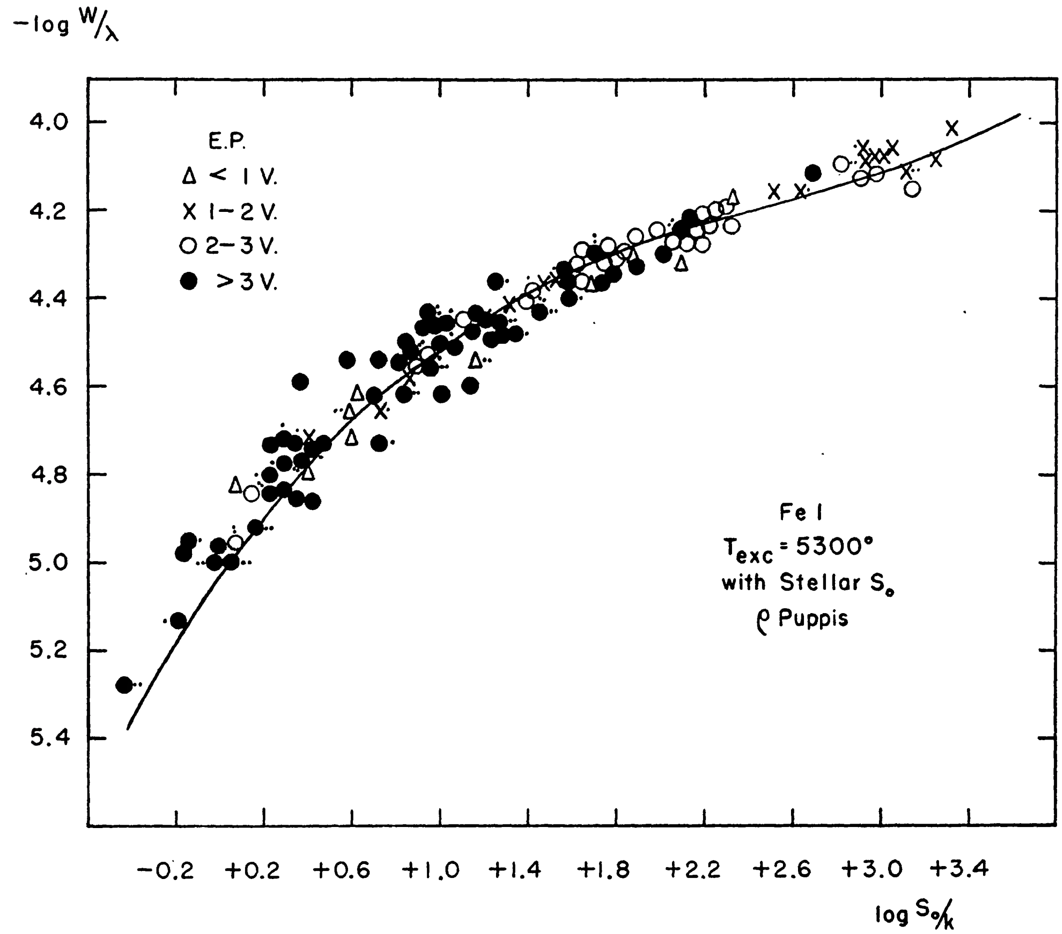

FIG. 6.—The curve of growth for Fe I in ρ Pup with the $\eta_0'(\tau)$ of Table 2 as abscissae. Note how the use of stellar values of line strengths reduces the scatter when compared to Fig. 4.

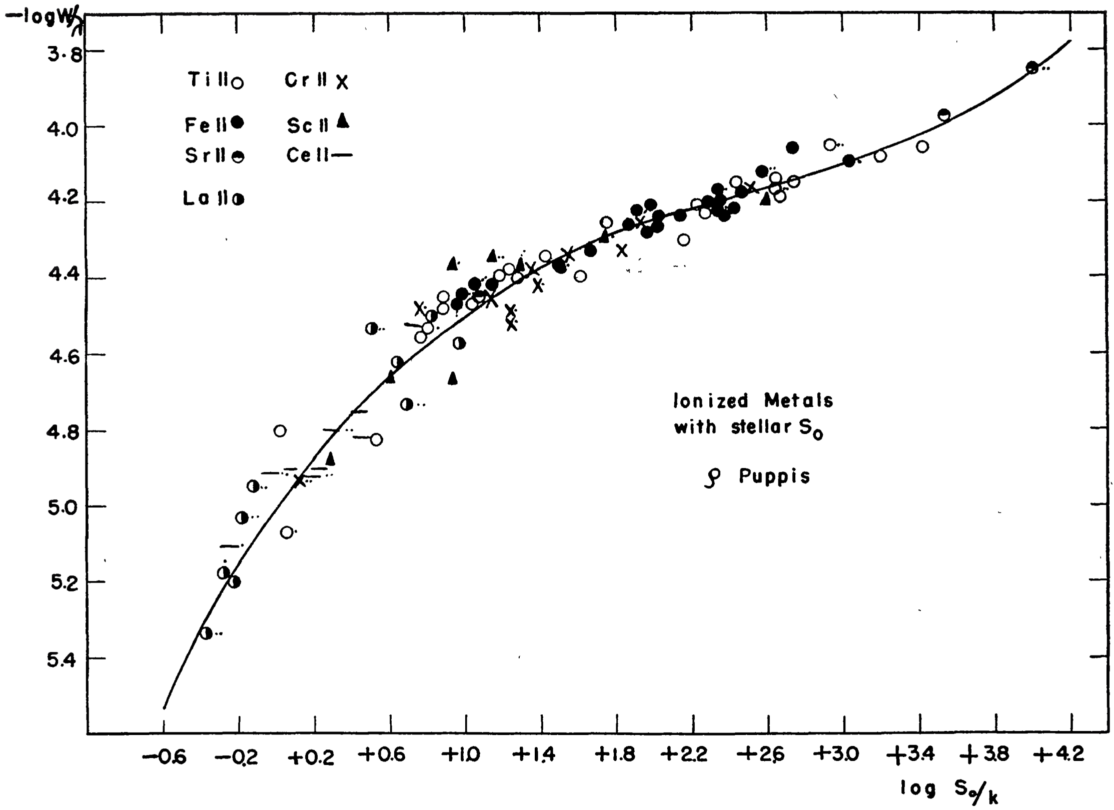

FIG. 7.—The curve of growth for other elements in ρ Pup based on the stellar $\eta_0'(\tau)$. Compare with Fig. 5.

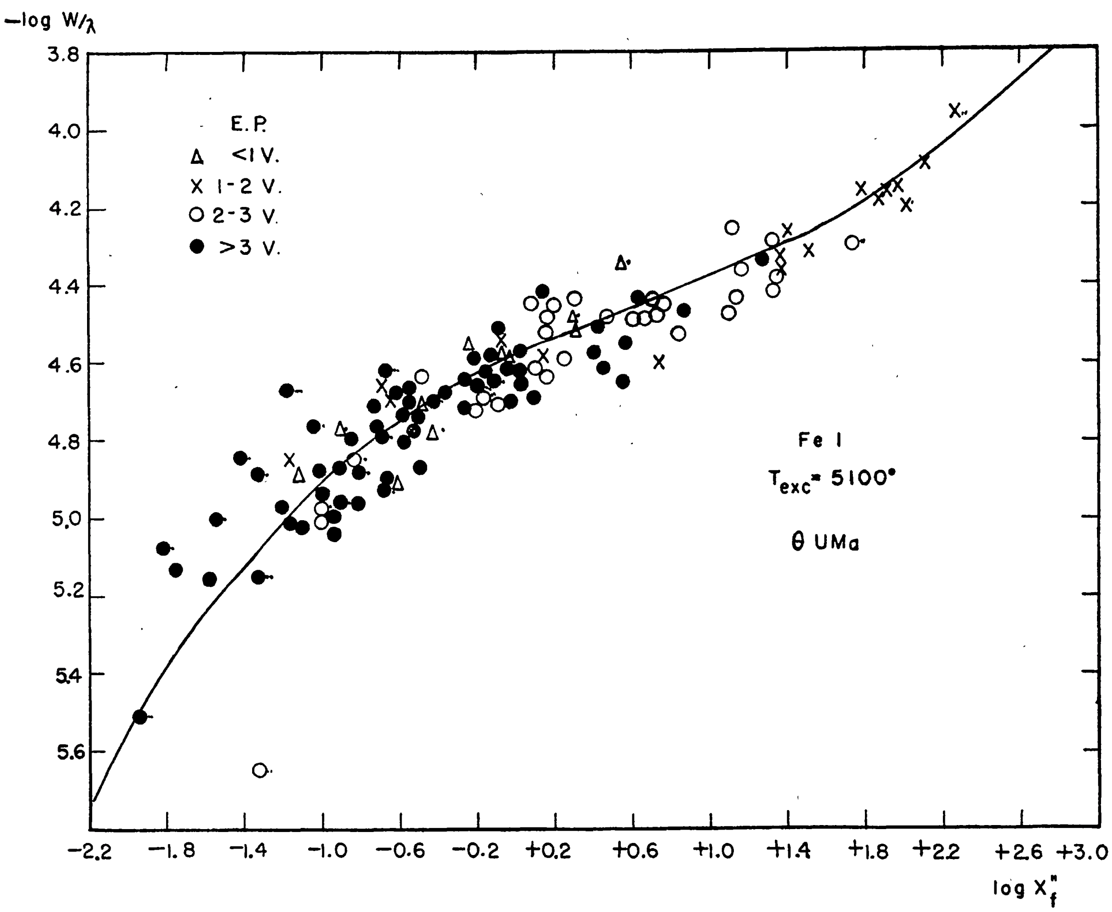

FIG. 8.—The curve of growth of *Fe* I in the giant θ UMa, using solar X_f''

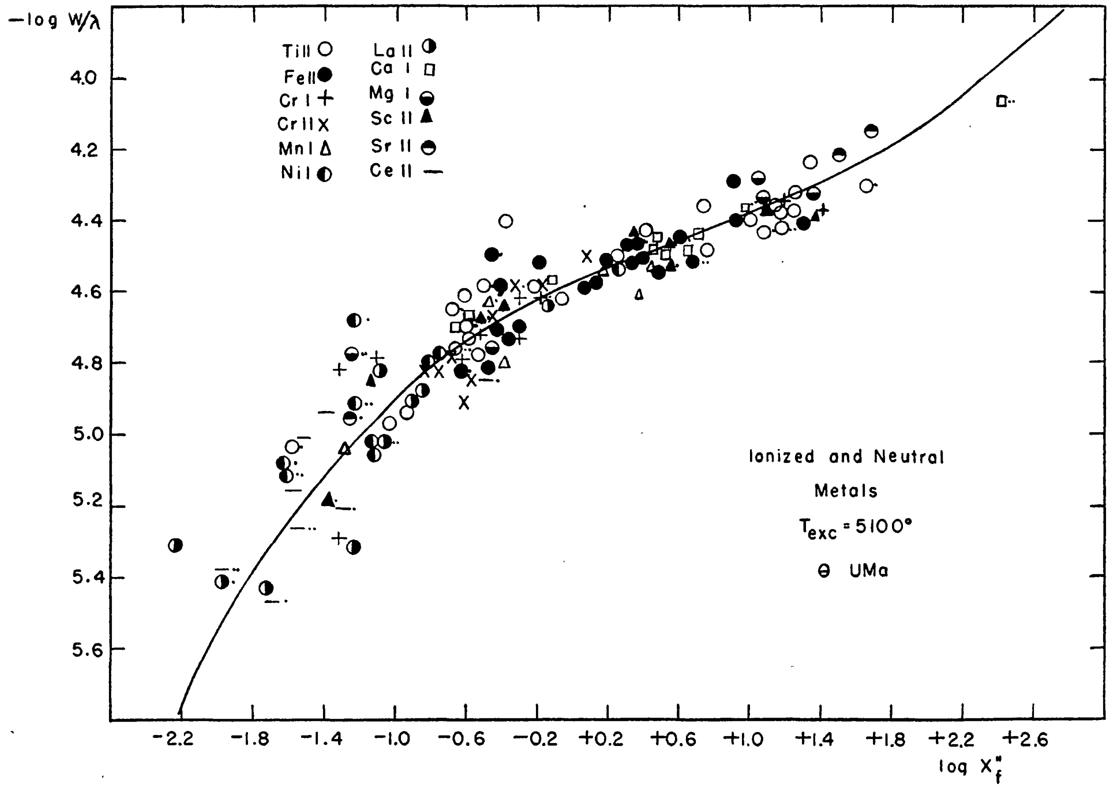

FIG. 9.—The curve of growth of other elements in θ UMa, using solar X_f''

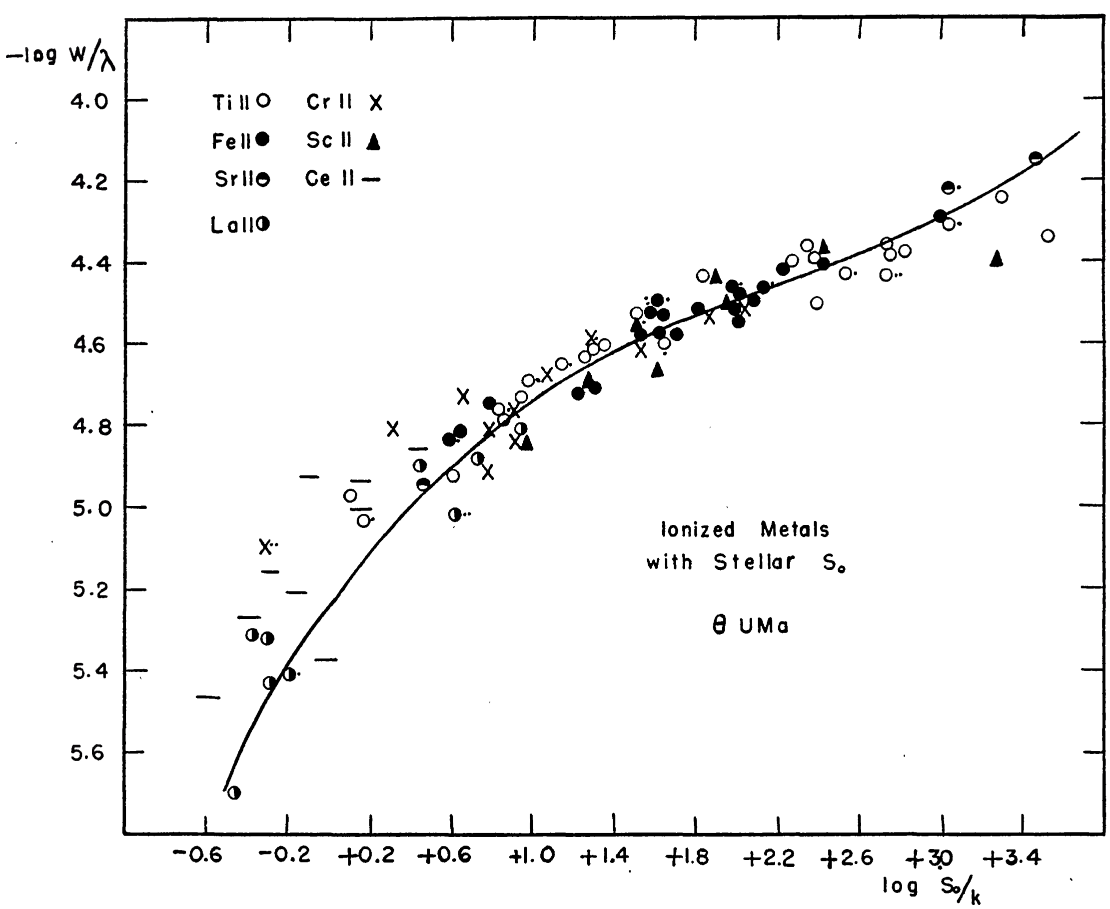

FIG. 10.—The curve of growth for ionized metals in θ UMa, using the stellar $\eta_0'(\tau)$. Compare with Fig. 9

by ionized lines of *Y* II, *Fe* II, and *Cr* II. In Plate 31 of the *Atlas* it can be seen that the variations of λ 4172, λ 4178, form one of the most striking luminosity effects in F0 stars. Detailed studies of blending effects, of the type suggested by Pannekoek and van Albada,[16] should prove important in the prediction of low-dispersion spectral and luminosity criteria.

THE PARAMETERS OF THE STELLAR ATMOSPHERES

The major problem of this investigation can be stated as follows: Does the change of curve of growth, temperature, and pressure from star to star completely account for all the changes of line intensity? Or are there actual changes in the abundances of the elements? Since we lack *f*-values for most lines, we evaluated all apparent abundances in terms of the solar abundance of the element in Table 7. These apparent abundances still involve the level of ionization and opacity. The most fundamental approach is that taken by Strömgren in the solar atmosphere, where with a detailed solar model the absolute intensities of certain lines were predicted. For the general investigation of the F stars, the data required for the construction of the model stellar atmospheres is almost completely lacking; only one star has an accurately known mass and luminosity. Eventually the parameters required for such models may be estimated. For example, the color temperature–effective temperature relation will be available from computations by Münch based on the continuous-absorption coefficients of H and H^- (given by Chandrasekhar and Breen[19] and by Chandrasekhar and Münch[20]) and the six-color photoelectric photometry of bright stars. For stars of high luminosity it may not be possible to use the gravitational value of the surface gravity if other mechanisms contribute to the support of these extended atmospheres. The Balmer discontinuity and the color temperatures will ultimately determine both the effective temperature and the electron pressure.

Meanwhile, we must proceed by indirect spectroscopic methods, based on a rough analysis of the star. We shall consider the level of ionization at a representative point in the stellar atmospheres, $\tau_0 = 0.25$; at this point $\theta_{\text{ion}} = 1.10\,\theta_e = 0.92\,\theta_0$. We compare the relative level of ionization of various elements in the star and in the sun. Since we have a model for the solar atmosphere, we know $\theta_{\text{ion}}(\odot) = 0.95$, $\log P_e(\odot) = 0.80$. (These values differ slightly from Strömgren's and fit better with the newer H^- absorption coefficients.) Therefore, in principle, two elements of different ionization potentials, observed in two stages of ionization, determine both $\theta_{\text{ion}}(*)$ and $P_e(*)$. The ionization equation is

$$\log \frac{N_r\,(*)}{\Sigma N\,(*)} - \log \frac{N_r\,(\odot)}{\Sigma N\,(\odot)} = K_r\,(\theta_{\text{ion}}) - \log P_e\,. \tag{30}$$

The ΣN is taken over all stages of ionization. Unfortunately, the simultaneous solution of two relations like equation (30) proves almost indeterminate. In fact the application of equation (30) to the observations results in a single approximately linear relation of the form:

$$\log P_e + c_2 \theta_{\text{ion}} = c_1\,, \tag{31}$$

where c_1 depends on the observed $\Delta \log \zeta_i$ and where c_2 is nearly independent of the ionization potential, averaging close to 9.0. While many elements of quite different c_2 and c_1 are observed in a single stage of ionization, in this investigation such elements cannot be used to determine θ_{ion} and P_e, since possible abundance variations from star to star cannot be excluded. In equation (30), even if an element has a gross abundance change from sun to star, both stages of ionization are affected, and no error is introduced.

The actual determination of the level of ionization was carried through for the following elements: *Fe* I/*Fe* II (wt. 2), *Cr* I/*Cr* II (wt. 1), *Ti* I/*Ti* II (wt. 1). The level of ioniza-

[19] *Ap. J.*, **104**, 430, 1946.

[20] *Ap. J.*, **104**, 446, 1946.

tion at the standard point, $\tau_0 = 0.25$, was known in the sun; the $\Delta \log \zeta_i(*)$ gave the ionization in the star, neutral element divided by total. Tables 8 and 9 give the results of these computations. Note in Table 9 the agreement of the observationally determined $\log P_e$ for the three elements. Note also how small the difference between the rate of change of P_e with θ is for *Fe* I and *Cr* I; the constants c_2 in equation (31) are 9.1 and 8.2, respectively.

To obtain a second relation between θ_{ion} and P_e, we make another type of assumption, which would permit changes of relative abundances of various metals to be determined, although not immediately giving their abundances relative to hydrogen. Let us assume that a certain group of heavy elements has the same fractional abundance per gram of

TABLE 8

IONIZATION OF STANDARD ELEMENTS

Element	$\log \frac{N_{\text{I}}(\odot)}{\Sigma N(\odot)}$	Observed Stellar Ionization $\log \frac{N_{\text{I}}(*)}{\Sigma N(*)}$				
		τ UMa	ρ Pup	θ UMa	α CMi	α Per
Fe I	−1.00	−2.80	−2.58	−1.99	−2.21	−3.00
Cr I	−1.86	−3.36	−3.04	−2.63	−2.66	−3.50
Ti I	−1.98	−3.19	−3.32	−2.66	−3.12	−3.51

TABLE 9

DETERMINATION OF LOG P_e FROM STELLAR IONIZATION

Star	$\theta_{\text{ion}}=0.7$				$\theta_{\text{ion}}=0.8$				$\theta_{\text{ion}}=0.9$			
	Fe I	*Cr* I	*Ti* I	Mean	*Fe* I	*Cr* I	*Ti* I	Mean	*Fe* I	*Cr* I	*Ti* I	Mean
τ UMa	+1.24	+1.32	+1.63	+1.35	+0.31	+0.50	+0.80	+0.48	−0.60	−0.31	−0.01	−0.38
ρ Pup	+1.46	+1.64	+1.50	+1.51	+0.53	+0.82	+0.67	+0.64	− .38	+ .01	− .14	− .22
θ UMa	+2.05	+2.05	+2.16	+2.08	+1.12	+1.23	+1.33	+1.20	+ .21	+ .42	+ .52	+ .34
α CMi	+1.83	+2.02	+1.70	+1.84	+0.90	+1.20	+0.87	+0.97	− .01	+ .39	+ .06	+ .11
α Per	+1.04	+1.18	+1.31	+1.14	+0.11	+0.36	+0.48	+0.26	−0.80	−0.45	−0.33	−0.60

stellar material in all stars and in the sun. Any gross change of A, the ratio of hydrogen to the metals, invalidates this assumption. The standard elements, together with weighting factors adopted, were: *Ti*(4), *V*(1), *Cr*(2), *Fe*(4), *Ni*(1), *Y*(1), *Ba*(1). These elements prove to be completely in the singly ionized state in F stars. (In τ UMa, *Ti* and *V* were omitted because of their possible slight weakening in that star.) In the analysis of the sun[8] A is equal to the ratio P_g/P_e, since the electrons are contributed by the metals. In the F stars hydrogen is about 1 per cent ionized and provides the electrons; then P_g/P_e varies as P_e. A change of A does not affect P_g/P_e or the opacity and would remain undetected in the following analysis until the absolute strengths of the hydrogen lines were predicted.

We find that the opacity of H and H^- in these stars is a slow function of temperature and nearly proportional to P_e. From the observed $\Delta \log \zeta_i$ for the singly ionized standard elements we obtain a mean ratio of $\log \kappa_\nu(*)/\kappa_\nu(\odot)$ and evaluate $\kappa_\nu(*)$. With a fair degree of approximation we write

$$\log P_e + \phi(\theta) = \log \kappa_\nu , \qquad (32)$$

where $\phi(\theta)$ is nearly a constant. A simultaneous solution of equations (31) and (32) proves highly determinate; the effects of observational errors in the final solution are

$$\Delta\theta_{\text{ion}} \approx 0.1\Delta c_1 - 0.1\Delta \log \kappa_\nu . \tag{33}$$

The observational errors are about ± 0.10 (m.e.) in both Δc_1 and $\Delta \log \kappa_\nu$, so that an error of ± 0.015 in θ_{ion} might be expected, with a corresponding error of ± 0.14 in $\log P_e$. The errors in the deduced $\log P_g$ and $\log g_e$ are about ± 0.30. However, while the internal agreement of different elements is good in the determination of $\log \kappa_\nu$, a larger systematic error may arise, owing to the errors of spectrophotometry. For example if our characteristic curve is in error so that all W's are increased by ϵ per cent, lines on the flat part of the curve of growth will give errors in the deduced η_0 of 2 to 4ϵ, appearing in full in κ_ν.

The theoretical κ_ν, including stimulated emission, is determined from the new H^- absorption coefficients of Chandrasekhar and his collaborators.[19, 20]. We evaluate and sum κ_ν at λ 4300 for the H^- absorption and the total H absorption, bound-free and free-free. Detailed tables of $\bar{\kappa}$ and $\kappa_\nu(H^-)$ are available elsewhere; the quantity $\kappa_\nu(H+H^-)$, required in this type of analysis, is given in Table 10. Note that electron scattering is not included; it would be appreciable in A stars and in supergiants and may slightly affect the results for α Per and τ UMa.

TABLE 10

LOG $\kappa_\nu(H + H^-)$

LOG P_e	θ					
	0.5	0.6	0.7	0.8	0.9	1.0
−2	−3.37	−3.05	−2.77	−2.69	−3.25	−3.36
−1	−2.37	−2.05	−1.84	−2.23	−2.51	−2.38
0	−1.37	−1.08	−1.19	−1.66	−1.55	−1.38
+1	−0.38	−0.24	−0.73	−0.75	−0.56	−0.38
+2	+0.53	+0.26	+0.07	+0.24	+0.44	+0.62
+3	+1.25	+0.88	+1.05	+1.24	+1.44	+1.62
+4	+1.74	+1.81	+2.04	+2.24	+2.44	+2.62

Table 11 gives the individual values of $\Delta \log \zeta_i$ for the standard elements in the ionized state. The level of ionization in F stars and in the sun is such that $\log \zeta_{\text{ion}}(*)/\zeta_{\text{ion}}(\odot)$ averages near $+0.02$. Since

$$\Delta \log \zeta_i = \log \frac{\dfrac{N(*)}{\kappa_\nu(*)}}{\dfrac{N(\odot)}{\kappa_\nu(\odot)}}, \tag{34}$$

$$\log \frac{\kappa_\nu(*)}{\kappa_\nu(\odot)} = +0.02 - \overline{\Delta \log \zeta_i \text{ (ions)}} . \tag{35}$$

(In some stars in Table 11 the elements Y II and Ba II show appreciable ionization.) The value of $\log \kappa_\nu(\odot) = -0.54$; from the mean $\Delta \log \zeta_i$ in Table 11 and from equation (35) we obtain the $\log \kappa_\nu(*)$ in the last row.

The rather complex curves relating $\log P_e$ and $\log \kappa_\nu$ were plotted for various θ; with $\log \kappa_\nu$ in Table 10 we read the $\log P_e$, for each θ, which gives the required opacity. A plot of the $\log P_e$ for each θ required by the ionization (Table 9) and now by the opacity gives θ_{ion} and $\log P_e$ as spectroscopically determined. These are given in Table 7; it is interesting to note that the θ_{ion} agree moderately well with each other and with the accepted stellar temperature scale and are appreciably smaller than θ_{exc}. This latter fact again suggests that the derived θ_{exc} are not very meaningful parameters of the stars. The detailed stellar models published by Strömgren and his collaborators[14] give the relation between P_g, P_e, and θ for various hydrogen abundances, A. Adopting $\log A = 3.8$, I find the spectroscopic values of P_g given in Table 7. The values of $\bar{\kappa}$ adopted by Strömgren differ slightly from those recently derived by Chandrasekhar, and the range of Strömgren's stellar models is too limited for us to proceed to evaluate the surface gravity exactly. Without exact models, an approximate method can be adopted. Since P_e/P_g is very roughly constant,

$$\frac{\bar{\kappa}(\tau)}{\bar{\kappa}(\tau_0)} = \frac{P_g(\tau)}{P_g(\tau_0)} . \qquad (36)$$

TABLE 11

EVALUATION OF STELLAR OPACITY

Element	Weight	$\Delta \log \zeta_i$				
		τ UMa	ρ Pup	θ UMa	α CMi	α Per
Ti II	4	....	+0.77	+0.54	+0.71	+0.94
V II	1	....	+0.63	+ .30	+ .70	+0.79
Cr II	2	+1.20	+0.88	+ .49	+ .57	+1.35
Fe II	4	+1.20	+1.06	+ .56	+ .98	+1.36
Ni II	1	+0.90	+0.50	+ .40	+ .20	+0.77
Y II	1	+0.99	+1.07	+ .45	+ .55	....
Ba II	1	+0.77	+0.55	+0.23	0.00	....
Mean	....	+1.10	+0.84	+0.48	+0.66	+1.12
$\log \kappa_\nu(*)$	....	−1.62	−1.36	−1.00	−1.18	−1.64

From the hydrostatic equation,

$$\frac{dP_g}{d\tau} = \frac{g_e}{\bar{\kappa}(\tau)} , \qquad (37)$$

we obtain

$$g_e = \frac{P_g(\tau_0)\,\bar{\kappa}(\tau_0)}{2\tau_0} . \qquad (38)$$

In this range of temperature, I find that $\log \kappa_\nu/\bar{\kappa} \approx -0.2$, from the tables of Chandrasekhar and Münch.[20] By choosing the representative point at $\tau_0 = 0.25$, as before, the g_e given in Table 7 are evaluated from purely spectroscopic data. Any agreement with the expected gravitational values of g, given in the last line of Table 7, is of considerable significance, since it justifies the assumptions made as to the abundance of the metals with respect to hydrogen. The gravitational g are approximately estimated from the masses, luminosities, and temperatures of the F stars. Systematically, $g_e < g$; this is expected for the supergiants, and it is interesting to note that the dwarf τ UMa, in spite of being 6 mag. fainter than ρ Pup, has a lower g_e than that star. This unexpected discrepancy is in line with the large turbulent velocity found for τ UMa (4 km/sec); no dwarfs had previously been found with appreciable turbulence. Another peculiar case is θ UMa, which has a relatively large g_e compared to α CMi, although of about the same luminosity. The weakness of all lines in θ UMa demands the high κ_ν and the consequently large g_e derived. Criticism of the g_e can be made on both observational and theoretical grounds; photometric errors affect κ_ν directly, and in stars like α CMi the variation of P_g and g with P_e is very steep. Errors of ± 0.3 in the log g_e may be expected.

OBSERVED RELATIVE ABUNDANCES OF THE ELEMENTS

In Table 7 we have tabulated the parameters of the atmospheres required to discuss the relative abundances of the elements. With θ_{ion}, P_e, and κ_ν determined from a small group of standard elements, we compute the level of ionization of all other elements. For each atom of type i in state of ionization r, we write the predicted values of the apparent abundances,

$$\Delta \log \zeta_{i,\,r} = \log \frac{N_{i,\,r}(*)}{\sum_r N_{i,\,r}(*)} - \log \frac{N_{i,\,r}(\odot)}{\sum_r N_{i,\,r}(\odot)} - \log \frac{\kappa_\nu(*)}{\kappa_\nu(\odot)} + \log \frac{z_i(*)}{z_i(\odot)}\,. \quad (39)$$

The quantity $z_i(*)/z_i(\odot)$ represents the abundance ratio, the number of atoms of the element i per gram of material in the star as compared to that ratio in the sun, i.e.,

$$z_i \equiv \sum_r N_{i,\,r}\,. \quad (40)$$

If the elements were present in the stars and the sun in the same proportions, all relative abundances $z_i(*)/z_i(\odot)$ would equal unity. From the observed $\Delta \log \zeta_i(*)$ listed in Table 7 and the ionization at θ_{ion} and P_e, equation (39) gives the values of $z_i(*)/z_i(\odot)$ computed for those elements for which the data seem trustworthy. (The results for α Per should throughout be considered of relatively low weight.) If the ionization has been correctly determined, the values of the abundances should be the same in both stages of ionization. This is obvious if there is a true abundance change; it is also true if some peculiar mechanism should ionize an atom, say *Ca* II, more heavily than is predicted by the Saha equation. The ratio *Ca* II/*Ca* I would not be affected by the same mechanism, and *Ca* I would be reduced in the same proportion as *Ca* II; *Ca* would be mainly in the unobservable stage of *Ca* III.

For reasons previously discussed, it was necessary to permit arbitrary zero points, α, in the $\Delta \log \zeta_i$ for *Mg*, *Ca*, *Mn*, *Ni*, and *Eu*. In the first four cases we evaluate these α by requiring that in the mean of the five stars the values of log $z_i(*)/z_i(\odot)$ should agree for the neutral and ionized elements. This adjustment remains as an unfortunate feature of the abundances of these elements in Table 7. The values determined, $\alpha_1 = -1.7$, $\alpha_2 = +0.74$, $\alpha_3 = +0.9$, $\alpha_4 = +.0.75$, are used in the final log $z_i(*)/z_i(\odot)$ given in Table 12. The case of *Ca* II may be taken as typical. The observational difficulties have been described. In the sun the collisional damping constant of the K line agreed with the damping found for the average metallic lines in the analysis of the curve of growth. The F stars may not show the same equality, and the deviation observed is in the sense that the K line is too weak in all F stars as compared to the sun. Before adjustment, the abundances of *Ca* indicated by *Ca* II and *Ca* I were as shown in the accompanying tabulation. The systematic nature of the required correction is obvious. (The results for τ UMa

	τ UMa	ρ Pup	α Per	θ UMa	α CMi
Ca I	−1.11	−0.15	0.0	+0.07	+0.25
Ca II	−1.80	−0.97	−0.6	−0.63	−0.63
Difference	−0.69	−0.82	−0.6	−0.70	−0.88

show the great weakening of *Ca* in that star.) It would have been possible to adjust *Ca* I to agree with *Ca* II, but then a large mean negative value of the *Ca* abundance would have resulted. Since the analysis of the K line is subject to greater uncertainties, the adjustment of *Ca* II seems reasonable. In the cases of *Mg* II and *Mn* II the solar X_f is suspect because of the high excitation potential involved. The case of *Ni* II is unsatisfactory; it was adjusted to give an abundance in agreement with *Ni* I, but the mean

TABLE 12

THE RELATIVE ABUNDANCES OF THE ELEMENTS IN UNITS OF THE SOLAR ABUNDANCE LOG $z_i(*)/z_i(\odot)$

Element	Z	τ UMa	ρ Pup	α Per	θ UMa	α CMi	Qual.	I.P. Volts	
Mg I	......	−0.8	−0.3	−0.2	+0.01	+0.34	a	....	....
Mg II	......	−0.9	− .2	− .2	+ .34	− .14	d	....	....
Mg	12	−0.85	− .25	− .2:	+ .12	+ .18:	b	7.61	14.97
Ca I	......	−1.06	− .15	.0	+ .07	+ .25	a	....	....
Ca II	......	−0.95	− .23	+ .1	+ .11	+ .11	d	....	....
Ca	20	−1.05	− .19	+ .05	+ .09	+ .18	b	6.09	11.82
Sc II	21	−1.65	− .79	− .4:	− .11	− .23	b	....	12.8
Ti I	......	−0.30	− .02	+ .08	+ .24	− .05	a	....	....
Ti II	......	−0.61	− .05	− .14	+ .08	+ .07	a	....	....
Ti	22	−0.45	− .04	− .03	+ .16	+ .01	a	6.81	13.6
V I	......	−0.72	− .50	− .7	− .37	− .57	b	....	....
V II	......	−0.52	− .19	− .5	− .43	+ .06	b	....	....
V	23	−0.62	− .35	− .6:	− .40	− .25	b	6.71	14.1
Cr I	......	+0.13	+ .24	+ .2	+ .09	+ .14	a	....	....
Cr II	......	+0.12	+ .06	+ .14	+ .03	− .07	b	....	....
Cr	24	+0.13	+ .18	+ .16	+ .07	+ .07	a	6.74	16.6
Mn I	......	+0.01	− .07	+ .3	− .04	+ .24	a	....	....
Mn II	......	−0.18	+ .08	+ .3	+ .34	− .14	d	....	....
Mn	25	−0.05	− .02	+ .3:	+ .09	+ .11	b	7.40	15.6
Fe I	......	−0.12	+ .10	.00	− .01	+ .19	a	....	....
Fe II	......	+0.12	+ .24	+ .27	+ .10	+ .34	a	....	....
Fe	26	0.00	+ .17	+ .14	+ .05	+ .26	a	7.86	16.16
Co I	27	−0.25	− .26	− .3:	− .28	− .08	b	7.85	17.1
Ni I	......	+0.63	+ .60	+ .3	+ .31	+ .37	b	....	....
Ni II	......	+0.57	+ .43	+ .3	+ .69	+ .32	c	....	....
Ni	28	+0.61	+ .54	+ .3:	+ .50	+ .35	c	7.61	18.4
Zn I	30	+0.58	+ .55	+ .1	+ .25	+ .20	b	9.35	17.89
Sr II	38	−0.26	+ .14	− .1	− .44	− .11	b	....	10.98
Y II	39	+0.06	+ .38	+ .2:	+ .03	− .03	a	....	12.3
Zr II	40	−0.90	− .13	− .3:	− .31	− .28	a	....	13.97
Ba II	56	+0.2	+ .2	− .3	− .07	− .62	b	....	9.96
La II	57	−0.06	− .04	− .1:	− .11	− .27	a	....	11.38
R.E. II	58–64	0.00	− .03	.0:	− .02:	− .55:	b	....	11.4
Eu II	63	+0.9	+0.8	+0.1:	0.0	+0.2	d	....	11.21

residual is left positive in all F stars. The excitation potentials of both *Ni* I and *Ni* II are higher than average.

The final abundances are given in Table 12. The rare earths (except *Eu* II) are lumped together as "R.E. II." Where both stages of ionization are available, the third entry for each element is the adopted mean abundance. The column headed "Z" gives the atomic number of the element; "Qual." measures the reliability of the determination, on a scale from "a," good, to "d," very poor. The last two columns give both first and second ionization potentials where relevant. In further discussion of the abundances in Table 12 we shall exclude τ UMa, which will be the subject of Paper III in this series; it apparently shows large abundance changes.

An error of excitation temperature will change some of the derived abundances. If the error of the difference $\theta_{exc}(*) - \theta_{exc}(\odot)$ were as large as 0.1, elements of excitation potential (E.P.) of 5 volts would have errors of log $z_i(*)/z_i(\odot)$ of 0.5. A weak correlation of abundance differences with excitation potential actually exists, in the sense that elements of high excitation potential have slightly higher abundances in the F stars. Actually, this correlation arises from the more striking low abundance of *Sr*, *Ba*, *Zr*, and *Sc*, which amounts to about −0.2. The lines of these elements have low excitation potential; they are known to be strong at the very low excitation temperatures of K and M giants. Such a low-temperature enhancement may already be present to a slight degree in the sun, because of a steep decrease of η with optical depth. If so, their apparently somewhat low abundance in F stars is unreal.

A curious effect is visible for *Zn* in Table 12; while only two lines are accessible, they are strong and unblended. All F stars show an abundance increase, largest in ρ Pup; in α Per, however, the lines are definitely weakened (to the eye as well), and the abundance is relatively low. Thus *Zn* I seems to show an absolute-magnitude effect with a maximum in the intermediate supergiants.

The element *Eu* II is particularly difficult. The strong lines at λ 4129, λ 4205, are badly blended in all stars, and in the supergiants almost hopelessly blended. All rare-earth lines are strong in ρ Pup, α Per, and τ UMa; and this strengthening is *normal*, not requiring any abundance changes. The strengthening of *Eu* II, however, seems somewhat excessive. A similar excessive strength for *Eu* II lines is noted by Hiltner[21] in β CrB, a peculiar F giant.

Except for τ UMa, it may be said that the four F stars show extremely small abundance changes from the sun. The spectroscopic differences between θ UMa and α Per are enormous to the eye, even on the lowest dispersion. Both differ even more strongly from the sun. Yet for about twenty elements in Table 12, there is no well-established difference of abundance of a factor of 2 between these stars. The accidental errors, especially in α Per, are quite large; to reduce their effect let us group the two "giants," ρ Pup and α Per, and the two "dwarfs," θ UMa and α CMi. Form the differences in abundance, giant divided by dwarf, i.e.,

$$\Delta \log z_i' \equiv \log \frac{\overline{z_i\,(\alpha \text{ Per}, \rho \text{ Pup})}}{z_i\,(\odot)} - \log \frac{\overline{z_i\,(\theta \text{ UMa}, \alpha \text{ CMi})}}{z_i\,(\odot)}. \tag{41}$$

Table 13 gives the mean value of these abundance differences between the F stars. A range of about 6 in absolute magnitude is involved. I have tabulated the elements in the order of their $\Delta \log z_i'$ in Table 13.

The total range of apparent abundance changes is of the order of ±0.30, and of this at least ±0.15 may be expected to be observational error. A very unexpected regularity appears in Table 13. The elements deficient in the supergiants are the lighter ones. The median atomic number, Z, is 23 for elements with negative residuals and 39 for those with positive residuals. If real, elements heavier than *Ni* are about 50 per cent more abundant in the supergiants than in the dwarfs and the lighter elements are 50 per cent less abundant. This small difference may have still another origin than in true abundance differences, since lighter elements have, on the average, lower ionization potentials and higher excitation potentials than do the heavy ones.

If the stars are grouped in the same way and are compared to the sun, no systematic effect in atomic weight is apparent. The straight mean log $z_i(*)/z_i(\odot) = -0.01$ for the giants and −0.03 for the dwarfs. These near-approaches to zero difference between the stars and the sun are only in part forced on the data by the method of reduction. The opacities are determined essentially by the strength of *Ti* II, *Cr* II, and *Fe* II, and the derived abundances of the other elements might well have differed greatly from the solar

[21] *Ap. J.*, **102**, 438, 1945.

values. There is a slight tendency toward positive residuals in the dwarfs for the light-elements. There are many observational and theoretical uncertainties involved, but the predominant evidence shows only small abundance variations of the heavier elements among the "normal" stars of a wide range of luminosity. The abundance of the heavy elements with respect to hydrogen will be treated separately, but a normal value is indicated by the nearly zero mean value of log $z_i(*)/z_i(\odot)$.

THE HYDROGEN ABUNDANCE

The hydrogen lines are subject to Stark and collisional broadening; because of the high excitation involved, their broadened wings are produced at large depths, and η increases with τ. With detailed model atmospheres, the prediction of the complete line contour can be carried out. If the lines near the Balmer series limit could be observed in F stars as they are in B and A stars, the point of disappearance of individual high series members could be used to estimate P_e. In B and A stars the run of W with series number is also used to estimate the number of excited atoms of hydrogen. Neither method can be applied to F stars, since lines beyond $H\zeta$ are blended with metallic lines. We require estimates of the hydrogen abundance accurate within a factor of 2, and the observational and theoretical difficulties may well produce a greater uncertainty.

TABLE 13

ABUNDANCE DIFFERENCES
SUPERGIANT/DWARF

$\Delta \log z_i'$	Element
< -0.30	*Mg, Sc*:
-0.29 to -0.20	*Ca*
$-.19$ to $-.10$	*Ti, Co*:
$-.09$ to $.00$	*V*:, *Mn, Fe, Ni*
$+.01$ to $+.10$	*Cr, Zr, Zn*
$+.11$ to $+.20$	*La*
$+0.21$ to $+0.30$	*Sr, Y, Ba, Eu*, rare earths

After some consideration it is apparent that the contours of $H\gamma$ and $H\delta$, available for our F stars, can determine the hydrogen abundance. The equivalent widths of these strong lines cannot be interpreted directly. The type of model atmosphere differs from star to star; the source of broadening may change from collisional damping to Stark effect. If the model changes, a line absorption at distance $\delta\lambda$ from the center of the line $A(\delta\lambda)$ may involve different $\eta(\delta\lambda)$ from star to star. Such an effect should be smallest in the wing of the line. In the wing we also know that Stark effect dominates unless the collisional damping is many times the radiation damping. In the wings the Stark broadening gives a line-absorption coefficient of

$$l(\delta\lambda) = C N_2 P_e T_e^{-1} (\delta\lambda)^{-5/2} , \qquad (42)$$

where C is given by the theory of the Stark effect and N_2 is the number of excited hydrogen atoms in the second level. Let us compute η in the star and the sun at wave lengths $\delta\lambda(*)$ and $\delta\lambda(\odot)$:

$$\frac{\eta[\delta\lambda(*)]}{\eta[\delta\lambda(\odot)]} = \frac{P_e(*)}{P_e(\odot)} \frac{T_e(\odot)}{T_e(*)} \frac{N_2(*)}{N_2(\odot)} \frac{\kappa_\nu(\odot)}{\kappa_\nu(*)} \left(\frac{\delta\lambda(\odot)}{\delta\lambda(*)}\right)^{5/2} . \qquad (43)$$

Our assumption is that the star and the sun follow the same model and that therefore the same observed absorption in the wing of the line corresponds to the same η in star and sun. Measure the width of the line, $\delta\lambda$, in various stars at certain fixed values of the absorption A; our assumption requires that the left-hand side of equation (43) equal unity. Thus N_2 is determined, and an application of the Boltzmann formula gives the total number of hydrogen atoms, N_0. The abundance then is

$$\log \frac{z_H(*)}{z_H(\odot)} = + 10.16[\theta(*) - \theta(\odot)] + \frac{5}{2} \log \frac{\delta\lambda(*)}{\delta\lambda(\odot)} + \log \frac{\kappa_\nu(*)\,\theta(\odot)P_e(\odot)}{\kappa_\nu(\odot)\,\theta(*)P_e(*)} . \quad (44)$$

The ionization of hydrogen can be neglected. A fundamental difficulty is to decide at what optical depth to evaluate κ_ν, θ, and P_e for equation (44). Since κ_ν/P_e appears and $\kappa_\nu \propto P_e$, the pressure variation is unimportant. The temperature variation has a large effect, however; we may ask whether the ionization temperature at $\tau_0 = 0.25$ or the excitation temperature (which is usually low) should enter the first term in equation (44). Previous experience[7] has shown that the low excitation temperature found for the metals cannot apply to the hydrogen lines; Strömgren found in the sun[8] that the observed value of N_2 was consistent with the opacity and the hydrogen abundance when the temperature at a rather deep layer ($\tau_0 = 0.53$) was used. However, only the difference $\theta(*) - \theta(\odot)$ appears, and the uncertainties are correspondingly reduced. If η were independent of optical depth, the present analysis would be quite satisfactory. The model dwarf F star, when compared with the sun, in Table 6 fortunately showed only small differences arising from the change of model, except in the extreme wing of the line.

TABLE 14

HYDROGEN LINE WIDTHS AND THE ABUNDANCE OF HYDROGEN

Star	$\log \frac{\delta\lambda(*)}{\delta\lambda(\odot)}$ Observed	$\log \frac{\delta\lambda(*)}{\delta\lambda(\odot)}$ Predicted θ_{ion}	$\log \frac{\delta\lambda(*)}{\delta\lambda(\odot)}$ Predicted θ_{exc}	$\log \frac{z_H(*)}{z_H(\odot)}$ θ_{ion}	$\log \frac{z_H(*)}{z_H(\odot)}$ θ_{exc}
τ UMa	+0.62	+0.46	+0.62	+0.40	0.00
ρ Pup	+ .56	+ .63	+ .53	− .18	+ .08
θ UMa	+ .28	+ .41	+ .34	− .32	− .15
α CMi	+ .49	+ .49	+ .44	.00	+ .12
α Per	+0.57	+0.67	+0.39	−0.22	+0.45

In the application of this analysis of the contours we use the solar contour given in the Utrecht *Atlas*,[17] obtained at the center of the solar disk. The hydrogen lines weaken toward the limb; the observations of $H\gamma$ and $H\delta$ by Royds and Narayan[22] have been criticized by D. S. Evans.[23] While the absolute intensities of the former investigators may be in error, we adopt the scale of decrease toward the limb that they observe. Rather than compute the solar line in the integrated flux, I have arbitrarily weakened the hydrogen lines as observed in the *Atlas* by contracting the wave-length scale by 15 per cent (about -0.06 in $\log W$). The line widths (which range from 2 to 30 A) were measured at absorptions $A = 0.1$, $A = 0.2$, $A = 0.4$ in the sun and in the F stars (Table 4). The ratios $\delta\lambda(*)/\delta\lambda(\odot)$ should be constant and, in fact, do agree moderately well. An unweighted mean is given for each star in Table 14. If the hydrogen abundance is normal, equation (44) gives the predicted values listed in Table 14. Predictions are given in both cases, using the ionization or the excitation temperature. The last two columns give

[22] *Kodaikanal Obs. Bull.*, **109**, 375, 1936.

[23] *M.N.*, **100**, 156, 1939.

the hydrogen abundance deduced from equation (44), using the observed line widths. It is interesting to note that the mean observed ratios of line widths in Table 14 are close to the ratios of equivalent widths in Tables 3 and 4.

Although sensitive to the temperature adopted, the general run of predicted line widths agrees well with the observed values. Most gratifying is the predicted strength of the hydrogen lines in the F supergiants, in agreement with the observations. In the discussion of Table 4 we found that an approximate null absolute-magnitude effect is observed for hydrogen lines in the F stars. The prediction in Table 14 actually suggests that the hydrogen lines should be enhanced in the supergiants (as contrasted to A stars, where the Stark effect results in weakened hydrogen lines in the supergiants). We may hope that eventually the positive absolute-magnitude effect in late-type giants will also be explicable without recourse to deviations from thermodynamic equilibrium.

The scatter of the derived abundances is large; positive residuals have no physical reality, since hydrogen forms substantially all stellar material in the sun. In the mean the two giants show about the same abundance of hydrogen as in the sun. The giant θ UMa has abnormally weak hydrogen lines, probably correlated with the weakness of the metallic lines. Though we endeavored to explain the latter by a large opacity, the predicted hydrogen lines still remain too strong. This star requires further theoretical investigation. A converse small apparent excess of hydrogen may exist in τ UMa; our discussion in Paper III will show that the metallic-line A stars do have somewhat stronger hydrogen lines than their metallic-line type requires. The excitation temperature may be slightly higher in the metallic-line A stars than it is in normal F stars; such an effect may be correlated with the observed turbulence, unusual in dwarfs.

Neglecting these small deviations, we see that the hydrogen abundance in the F stars is compatible with that in the sun within a factor of 2. We have already shown that, on the whole, the metals show about the same relative abundances as in the sun. Large differences of absolute magnitude do not involve any gross changes of abundance. For the first time we may with some confidence say that the spectrum of a star could be predicted in detail from that of the sun. Since we have a satisfactory source of opacity, the color temperature, the Balmer discontinuity, and the absolute intensities of the lines of hydrogen and the metals are all predictable and, with the exception of the first two, have been now proved consistent with observation. One parameter of the stellar atmospheres which is not directly given by the theory is the turbulence, which for some unknown reason increases systematically from dwarfs to giants. With this is correlated abnormally low surface gravity. Only τ UMa, as a dwarf, has unusual turbulence and low surface gravity and shows several apparent abnormal abundances of the metals.

I wish to express my gratitude to Dr. S. Chandrasekhar and to Dr. B. Strömgren for their invaluable discussion of theoretical problems and to Dr. K. O. Wright for providing solar-line strengths in advance of publication.